Journal of Controlled Release 369 (2024) 163–178

Contents lists available at ScienceDirect

Journal of Controlled Release

journal homepage: www.elsevier.com/locate/jconrel

Poly(D,L-lactide-*co*-glycolide) particles are metabolised by the gut microbiome and elevate short chain fatty acids

Laura E. McCoubrey [a], Fabiana Ferraro [b], Nidhi Seegobin [a], Jérémy Verin [b], Haya A. Alfassam [a,c], Atheer Awad [a,d], Massimo Marzorati [e], Lynn Verstrepen [e], Jonas Ghyselinck [e], Julie De Munck [e], Jelle De Medts [e], Evi Steppe [e], Valerie De Vleeschhauwer [e], Gilles De Rocker [e], Alexandra Droesbeke [e], Melanie De Rijck [e], Sara Vanthoor [e], Frédéric Moens [e], Juergen Siepmann [b], Florence Siepmann [b], Simon Gaisford [a], Mine Orlu [a], Abdul W. Basit [a,*]

[a] *UCL School of Pharmacy, University College London, 29-39 Brunswick Square, London WC1N 1AX, United Kingdom*
[b] *Univ. Lille, Inserm, CHU Lille, U1008, F-59000 Lille, France*
[c] *Advanced Diagnostics and Therapeutics Institute, Health Sector, King Abdulaziz City for Science and Technology (KACST), 114422 Riyadh, Saudi Arabia*
[d] *Department of Clinical, Pharmaceutical and Biological Sciences, University of Hertfordshire, College Lane, Hatfield AL10 9AB, United Kingdom*
[e] *ProDigest BVB, Technologiepark 73, 9052 Ghent, Belgium*

ARTICLE INFO

Keywords:
PLGA
Microbiome medicine
Colonic drug delivery
Nanoparticles and microparticles
Metabolomics
Microbiome sequencing
Spray drying

ABSTRACT

The production of short chain fatty acids (SCFAs) by the colonic microbiome has numerous benefits for human health, including maintenance of epithelial barrier function, suppression of colitis, and protection against carcinogenesis. Despite the therapeutic potential, there is currently no optimal approach for elevating the colonic microbiome's synthesis of SCFAs. In this study, poly(D,L-lactide-*co*-glycolide) (PLGA) was investigated for this application, as it was hypothesised that the colonic microbiota would metabolise PLGA to its lactate monomers, which would promote the resident microbiota's synthesis of SCFAs. Two grades of spray dried PLGA, alongside a lactate bolus control, were screened in an advanced model of the human colon, known as the M-SHIME® system. Whilst the high molecular weight (Mw) grade of PLGA was stable in the presence of the microbiota sourced from three healthy humans, the low Mw PLGA (PLGA 2) was found to be metabolised. This microbial degradation led to sustained release of lactate over 48 h and increased concentrations of the SCFAs propionate and butyrate. Further, microbial synthesis of harmful ammonium was significantly reduced compared to untreated controls. Interestingly, both types of PLGA were found to influence the composition of the luminal and mucosal microbiota in a donor-specific manner. An *in vitro* model of an inflamed colonic epithelium also showed the polymer to affect the expression of pro- and anti-inflammatory markers, such as interleukins 8 and 10. The findings of this study reveal PLGA's sensitivity to enzymatic metabolism in the gut, which could be harnessed for therapeutic elevation of colonic SCFAs.

1. Introduction

The gut microbiome encompasses a hub of metabolic activity, whereby microbial and human metabolites interplay in a dynamic and bidirectional manner [1]. Small molecules produced by the intestinal microbiota have significant effects on host health. For example, indoles generated from bacterial tryptophan metabolism modulate the aryl hydrocarbon receptor within epithelial cells, safeguarding against inflammation and carcinogenesis [2]. Neuroactive compounds, such as serotonin and dopamine, are synthesised by bacteria in the GI tract and could play a role in human mood, motor control, sleep, and social behaviour [3].

SCFAs are an important group of microbial metabolites. Key SCFAs include acetate, propionate, and butyrate, and are produced through bacterial fermentation of dietary fibre in the colon. SCFAs activate cell-surface receptors such as free fatty acid receptor 3, succinate receptor 1, and hydroxycarboxylic acid receptor 2, leading to far-reaching effects on host physiology [1,4]. These effects include maintenance of epithelial

* Corresponding author.
E-mail address: a.basit@ucl.ac.uk (A.W. Basit).

https://doi.org/10.1016/j.jconrel.2024.03.039
Received 4 January 2024; Received in revised form 17 February 2024; Accepted 20 March 2024
Available online 26 March 2024

barrier function, suppression of colitis, immunoprotection (*e.g.*, against asthma), inhibition of carcinogenesis, cardiovascular protection, and improved glucose tolerance [1,5–8].

Insight into the roles of gut microbial metabolites in human health has sparked interest in their development as potential medicines [4,9]. Among them, SCFAs have garnered substantial attention and investment, with the therapeutic potential of butyrate reported as early as the 1970s [10]. However, despite this early interest, no licensed pharmaceutical products currently exist for delivery of SCFAs, either in their original or pro-drug form [11]. Key reasons for this may lie in the molecules' pungent odours and variability in clinical trials. An early clinical study reported that patients developed 'socially unacceptable odour' following injection with butyric acid, arising from the volatile compound's presence in sweat and breath [12]. Secondly, clinical studies delivering SCFAs have produced varying results, with common pitfalls including small sample sizes, heterogenous endpoints, different administration routes, and biopharmaceutical challenges (*i.e.*, achieving an effective concentration of drug in the colon) [13–15].

One notable success in SCFA delivery has been inulin-propionate ester (IPE), in which the SCFA propionate is covalently bound to the prebiotic inulin [16]. Upon arrival in the colon, the microbiota cleaves propionate from inulin and releases the SCFA at its target site [17]. Clinical studies have shown numerous benefits of IPE administration, including significant reductions in weight gain, intrahepatocellular lipid content, pro-inflammatory IL-8 in serum, and abdominal adipose tissue distribution in overweight and obese adults, alongside changes in faecal microbiome composition [17–19]. However, to exert these therapeutic benefits IPE must be administered in high dosages (10–20 g/day). Such dose sizes would increase the pharmaceutical burden on patients more than a typical oral dosage form providing <1.0 g of drug. An additional reason for the lack of translation of SCFAs as medicines could include their wide discussion in the literature, which may have impaired their patentability for pharmaceutical companies [20].

In light of these challenges, there is substantial opportunity for developing novel products that can increase colonic SCFA concentrations. The two most researched methods to increase colonic SCFA concentrations, without directly delivering SCFAs, include administration of prebiotics and probiotics [21–24]. As with IPE, one crucial drawback of prebiotics is their dose; to elicit a therapeutic effect they generally need to be administered in large doses, which may place undue administration burden on patients [25]. *Lactobacillus* and *Bifidobacteria* represent the most widely researched genera of probiotics [26,27]. They are typically formulated as solid oral dosage forms with live cell counts from 10^8 to 10^{10} CFU/mL and have been clinically tested for a wide range of indications, namely irritable bowel syndrome, inflammatory bowel disease (IBD), antibiotic-associated diarrhoea, *C. difficile* infection, obesity/metabolic syndrome, neuropsychiatric conditions, and atopic dermatitis [27–31]. Many strains within these genera can directly produce SCFAs or lactate as a precursor for microbial SCFA synthesis in the intestines (Fig. 1) [21,32]. Whilst probiotics have received promising results in a myriad of studies, they face multiple pharmaceutical and biopharmaceutical challenges. For instance, formulation processes

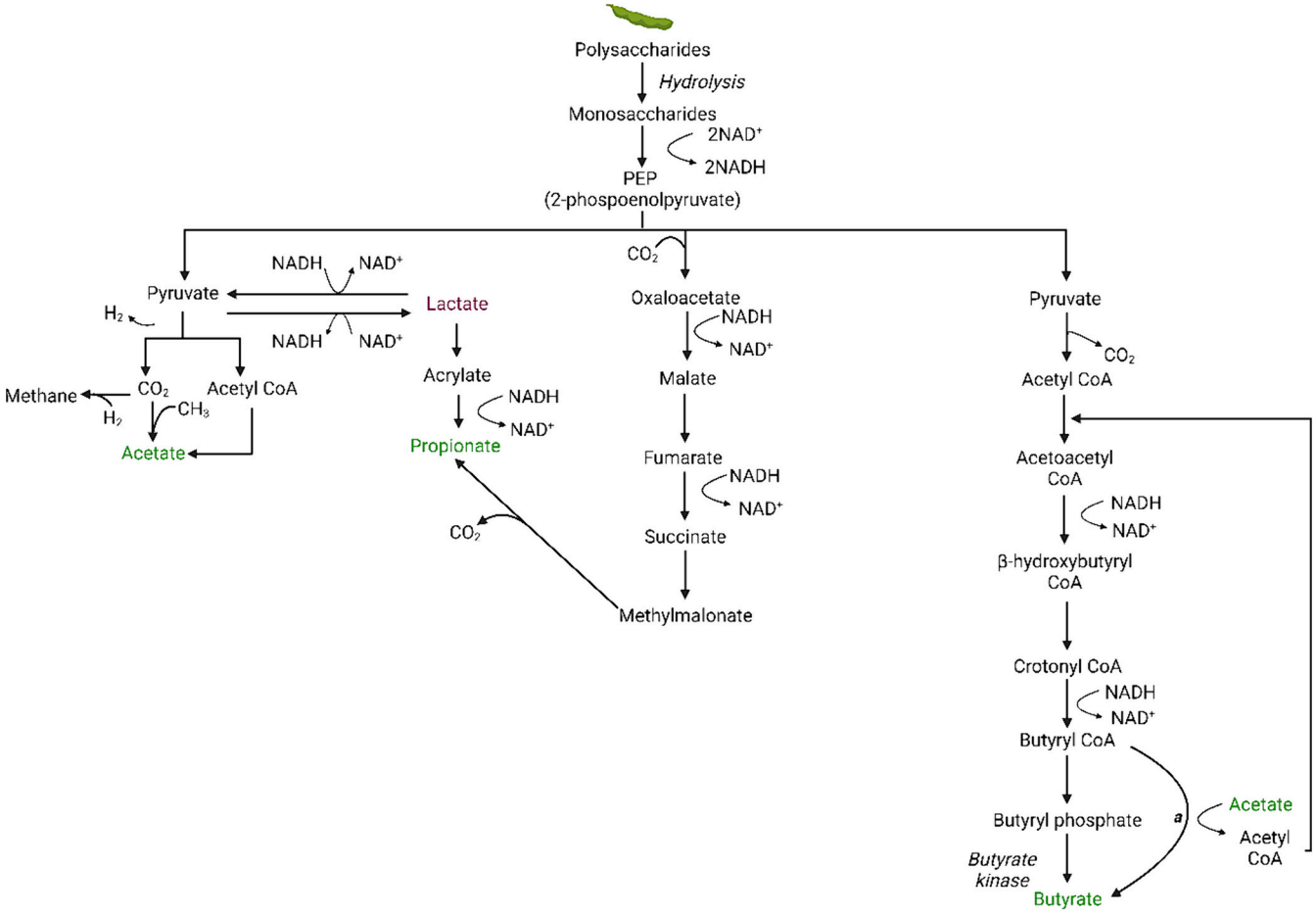

Fig. 1. The metabolic pathway detailing the fermentation of dietary carbohydrates to SCFAs by the colonic microbiota, with lactate highlighted as a key intermediatory. The enzyme '*a*' involved in the synthesis of butyrate represents butyryl CoA:acetate CoA transferase. A multitude of bacterial species are capable of producing SCFAs in the gut; for example, members of the Bacteroidota phylum are mainly responsible for producing acetate and propionate, whereas the Bacillota phylum is the predominant source of butyrate production [4]. Reference [36] provides a detailed overview of bacterial species involved in intestinal lactate production and utilisation. Figure revised from reference [4], which was published open-access under the Creative Commons Attribution License.

can frequently reduce the number of live bacteria within products due to heat, mechanical stress, oxygen, and excipient exposure [33]. Further, gastric acid, enzymes, and bile salts can inactivate probiotics *in vivo*, reducing the number of live bacteria that reach the colon [34]. Even probiotics that reach the colon alive can have insufficient effects due to lack of mucosal colonisation [35]. Hence, there is a requirement for alternatives to prebiotics and probiotics for augmentation of colonic SCFAs.

The aim of this study was to develop an oral therapeutic that could increase colonic SCFA concentrations. Two types of poly(D,L-lactide-*co*-glycolide) (PLGA) were selected and formulated as particles in the nano to micro range. It was hypothesised that the PLGA would be metabolised by the microbiota, resulting in significant and controlled liberation of lactate monomers, which would subsequently be utilised for SCFA synthesis (Fig. 1). PLGA was selected over poly(D,L-lactide acid) (PLA) due to its higher hydrophilicity, which could facilitate interaction with fluids *in vivo* [37]. The biocompatibility of PLGA is well documented for parenteral administration, thus toxicity following oral administration was judged to be unlikely [38]. The PLGA particles were evaluated using the M-SHIME® batch reactor, an advanced model of the human colon, to assess their potential for therapeutic modulation of the microbiome and colonic epithelium [39]. The results reveal previously unknown interactions between PLGA and the microbiome, which could open new avenues for treating microbiome-based disease.

2. Materials and methods

2.1. Materials

Resomer® RG 504H (PLGA, acid terminated, 50:50, Mw 38,000–54,000 g/mol), referred to as 'PLGA 1', and Resomer® Condensate RG 50:50 MN 2300 (PLGA, acid terminated, 50:50, Mw 2000–2500 g/mol), referred to as 'PLGA 2' were purchased from Evonik Industries (Essen, Germany). Pure lactic acid was purchased from Scientific Laboratory Supplies Ltd. (Nottingham, England). Caco-2 cells (HTB-37) were purchased from American Type Culture Collection (Virginia, US). Lipopolysaccharide (LPS) sourced from *Escherichia coli* K12 and THP1-Blue™ cells were purchased from InvivoGen (California, US). Where used, water was of HPLC-grade and obtained *via* an ELGA HPLC water purification system (ELGA LabWater, High Wycombe, England).

2.2. Methods

2.2.1. Spray drying of PLGA particles

The formulation of nano-microparticles was strategically chosen to maximise the polymers' surface area to volume ratio, thereby increasing the proportion of PLGA exposed to the microbiota. For this purpose, PLGA particles were prepared by spray-drying under anaerobic (nitrogen-rich) conditions. A BUCHI™ B-290 spray drier with a B-295 inert loop (BUCHI™, Flawil, Switzerland) was utilised with precise operating parameters to achieve desirable particle attributes. The inlet temperature was set to 50 °C, the aspirator was set to 95%, and the height was maximised (65 mm). PLGA was pumped through silicone tubing at a 10% pump rate *via* a two-fluid nozzle (Ø 0.7 mm, BUCHI™, Flawil, Switzerland). The feed concentration of PLGA in acetone was 50 mg/mL (5.0% *w/v*).

2.2.2. Scanning electron microscopy

Scanning electron microscopy (SEM) was used to determine the morphology and size of PLGA particles. A few milligrams of each sample were spread evenly onto a 25 mm aluminium stub using self-adhesive carbon tape (Taab Laboratory Equipment, Reading, England). To prepare the particles a fine layer of gold was sputtered onto the sample surface for 60 s at a current of 20 mA, using the Quorum Q150R Plus Rotary Pumped Coater (Quorum, Laughton, England). Examination of the particles was then conducted with the Phenom Pro Desktop SEM (Fisher Scientific, Loughborough, England) at an accelerating voltage of 10 kV. Images were captured digitally. Five batches of PLGA 1 and PLGA 2 were examined with SEM and 5–20 images of each batch were captured.

The size of particles was measured using ImageJ (version 1.53 t), *via* the line tool, with the scale set according to the scale bar shown in the SEM images. Individual particles were measured manually as automatic particle counting and sizing could not be reliably performed by the software due to the close proximity of particles. The largest and smallest particles (around five of each) within each image were visually selected and measured to provide insight into particle size distribution.

2.2.3. Set-up of the human colon model

The behaviour of PLGA particles in a simulated colonic environment was investigated using the M-SHIME® model, configured for short-term batch experiments [21,39]. These experiments were conducted at ProDigest (Gent, Belgium). The human colon model consisted of glass vessels inoculated with 70 mL sterile basal medium, 1.40 g/L mixed fibre, and 10% *v/v* faecal suspension. Here, the basal medium contained a proprietary mix of salts and nutrients similar to that used by Ghyselinck et al. [40]. To mimic the buffering capacity of the colon, the basal medium was adjusted to have the same biorelevant buffering capacity as fed state simulated colonic fluid [41]. Mixed fibre was present in the incubation medium to provide a carbon source for the faecal microbiota and to simulate a fed colonic state [42].

Faecal suspensions were added to the incubation medium to mimic the colonic microbiome and thus facilitate examination of PLGA's interactions with the microbiota. Faecal samples were collected from three healthy adult donors (no health conditions, no use of antibiotics in the preceding three months, $n = 2$ females, $n = 1$ male) and stored at −80 °C in aliquots. Ethical approval for collection of faecal samples was obtained from the University Hospital Ghent (reference number: B670201836585). Faecal suspensions (7.50% *w/v*) were prepared in an anaerobic environment by homogenising faecal samples with a buffer (K_2HPO_4 8.80 g/L; KH_2PO_4 6.80 g/L; sodium thioglycolate 0.10 g/L; sodium dithionite 0.015 g/L) and an in-house cryoprotectant; a modified version of that developed by Hoefman et al. [43].

A faecal suspension of 7.50% *w/v* is similar to the concentration shown by Vertzoni et al. to represent the metabolic activity of colonic bacteria (8.3% w/v, based on microbial depletion of four drugs) [44]. Faecal suspensions were thawed only once, immediately prior to addition to incubation vessels, to preserve microbial viability [45]. Five mucin-covered microcosms, as previously used by Ghyselinck et al. [46], were also added to each reaction vessel to enable simulation of the mucosal colonic microbiome, which is known to significantly differ from that of the lumen [47].

Spray-dried PLGA particles (PLGA 1 and 2) were incubated in vessels containing the faecal microbiota from each of the three healthy donors ($n = 3$ incubations per donor, hence $n = 9$ incubations per PLGA type). The PLGA dose was selected based on results from an initial dose-finding study, wherein ascending concentrations of PLGA particles were incubated in the M-SHIME® model with the faecal microbiota of a single human donor ($n = 1$ per concentration) (Fig. S1). A final dose of 4.5 g/L was chosen to prevent over-acidification of the media whilst maximising butyrate production. A bolus of lactic acid was used as a control in the dose-finding and main experiments to examine the difference between immediate lactate availability and controlled release of lactate from PLGA. The dose of the lactate bolus was selected to be equal to the number of moles of lactate in the PLGA samples (PLGA: 54% molar weight lactate, 46% molar weight glycolate). As with the PLGA incubations, lactate was incubated within vessels containing the faecal microbiota from each of the three donors ($n = 3$ incubations per donor). A blank medium (70 mL sterile basal medium, 1.40 g/L mixed fibre, and 10% faecal suspension) was used as an untreated control ($n = 3$ incubations per donor). This resulted in 36 incubations in the main 48-h

M-SHIME® batch experiment (Fig. 2).

Before commencement of the incubations the headspace of vessels was flushed with nitrogen (20 × 2 min cycles; 700 mbar overpressure, 900 mbar underpressure) to generate an anaerobic environment for microbial growth [48]. Incubations were conducted for 48 h with vessels maintained at 37 °C and continuously shaken at 90 rpm.

2.2.4. Deployment of the human colon model

2.2.4.1. Measuring fermentative activity. Samples from the M-SHIME® experiment were collected at 0, 3, 6, 24, and 48 h, enabling a thorough assessment of the dynamic changes over the incubation period. The pH of incubations was measured using a calibrated pH probe. Lactate concentration was assayed using a commercially available Enzytec™ kit (R-Biopharm AG, Darmstadt, Germany) with an LOQ of 10.0 mg/L, according to the manufacturer's instructions. Concentrations below this LOQ were set to zero. Concentrations of SCFAs and branched chain fatty acids (BCFAs), isobutyrate, isovalerate and isocaproate, were measured using gas chromatography (GC) coupled with flame ionisation detection (FID). Here, 2-methyl hexanoic acid was added as an internal standard and 2.0 mL of sample was extracted using diethyl ether. The GC-FID protocol utilised a GC SGE capillary column (30 mm × 0.32 mm ID-BP 21 × 0.25 μm (Achrom, Machelen, Belgium)) operating at a temperature range of 110–160 °C with an increase of 6 °C/min. The injection volume was set at 1.0 μL, the temperature of the injector and detector was 200 °C, and the carrier gas was nitrogen (95.6 mL/min). Ammonium concentration was measured with the indophenol blue method using an AQ300 Discrete Analyzer (SEAL Analytical, Wisconsin, United States) [49]. Gas production (including N_2, O_2, CO_2, H_2, CH_4, NH_3, H_2S, and volatile amino acids and SCFAs) was determined by measuring the pressure (kPa) in the headspace of each vessel with a pressure meter.

2.2.4.2. Profiling luminal and mucosal microbiome structure. The impact of treatments on the luminal microbiome structure was analysed by comparing the microbial composition and abundance of samples collected at 0 and 48 h. Quantitative bacterial taxonomic profiling was conducted by combining two experimental methods: 16S rRNA-targeted Illumina sequencing and flow cytometry, as in reference [50]. This combination of methods facilitated the assignment of microbial counts per taxonomic group. The absolute counts of taxonomic groups were calculated by multiplying the relative abundances measured during sequencing with the total viable cell count measured by flow cytometry.

Samples (n = 3 per donor per timepoint) taken from the lumen of incubation vessels were aliquoted into two separate groups for cell counting and Illumina sequencing.

The cell count of samples was measured using an Accuri™ C6 Plus Flow Cytometer (BD Biosciences, New Jersey, US) according to the method in reference [21]. Briefly, samples were diluted ten-fold in phosphate-buffered saline solution and cells were stained using SYTO 24 dye and propidium iodide. Cells were then passed through the cytometer at high flow rate and counted *via* detection of fluorescence. The BD Accuri CFlow software was utilised to analyse data. Signal noise, *e.g.*, arising from medium debris, was removed by applying a threshold value of 700 on the SYTO channel for all samples. Parent and daughter gates were set to count all bacterial populations accurately.

Samples were compositionally analysed using 16S rRNA-targeted Illumina paired-end sequencing. Cells were pelleted from 1.0 mL of luminal sample, DNA was extracted, and subsequently amplified following an in-house ProDigest protocol, as used in references [21, 40, 46]. For amplification, the QuantStudio 5 Real-Time PCR system (Applied Biosystems, Foster City, US) was used with primers that span two hypervariable regions (V3 - V4) of the 16S rRNA gene: 341F (5′-CCTACGGGNGGCWGCAG-3′) and 785R (5′-GACTACHVGGGTATC-TAAKCC-3′). Sequencing of the 2 × 250 base pair amplicons was completed by LGC genomics GmbH (Berlin, Germany) using the Illumina Miseq platform as per manufacturer's instructions [51]. To ensure data quality, read assembly and clean-up was completed by following the standard operating procedure for the mothur code (Version 1.44.3) developed by Kozich et al. [52]. This involved assembling reads into contigs, alignment-based quality filtering, removal of chimeras, and assignment of taxonomy into operational taxonomic units (OTUs) based on 97.0% sequence similarity. Sequences that were unclassified, classified as non-bacterial (*e.g.*, eukaryotic, archaeal, viral), or had relative abundances of <5% across samples were excluded from the analysis.

The mucosal microbiome was analysed with 16S rRNA-targeted Illumina sequencing without flow cytometry, to generate data in the form of relative OTU abundances. This process mirrored the sequencing method used for the luminal samples, wherein mucosal samples from the mucin-covered microcosms (0.1 g, n = 3 per donor per timepoint) were

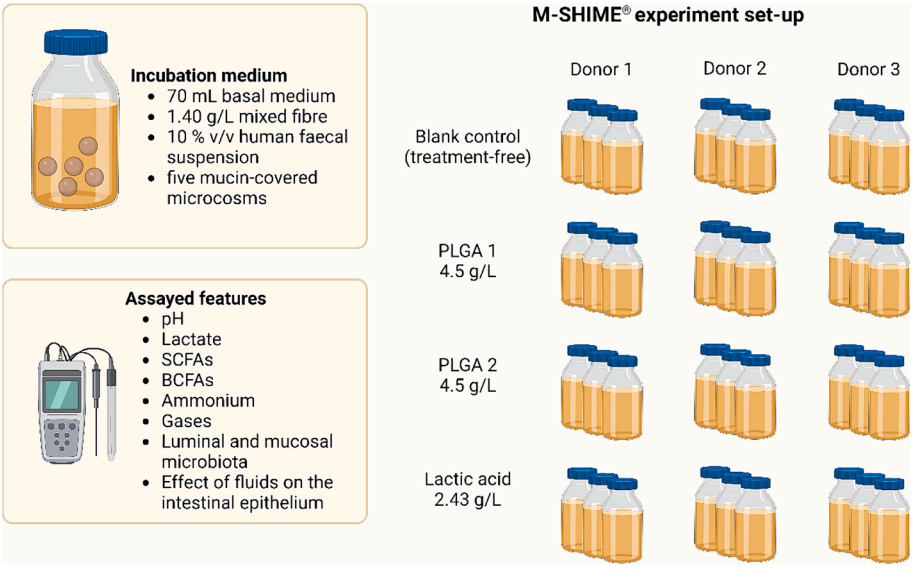

Fig. 2. Experimental setup of the main colonic simulation study. PLGA 1: high Mw PLGA (38,000–54,000 g/mol); PLGA 2: low Mw PLGA (2000–2500 g/mol). Samples were incubated in a short-term M-SHIME® system for 48 h with the faecal microbiota sourced from three healthy human adults (Donors 1 and 2: female; Donor 3: male). N = 3 incubations were conducted per donor for each sample (PLGA 1, PLGA 2, lactate, blank control (treatment-free)).

sampled.

2.2.4.3. Effect of treatments on the intestinal epithelium. The Caco-2/THP1 co-culture model was utilised to test the impact of treatments on an IBD-like intestinal epithelium. This co-culture model features an apical compartment comprised of Caco-2 cells that, when seeded on suitable supports, mature into enterocyte-like cells [53,54]. The exact method followed was first reported by ProDigest in reference [55]. The basolateral compartment of the model consists of THP1 monocytes, which differentiate into macrophage-like cells upon treatment with phorbol 12-myristate 13-acetate (PMA) [56]. In this study, THP1-Blue™ cells were used as these cells have been transfected with a secreted alkaline phosphatase (SEAP) gene. The secretion of SEAP in response to NF-κB activation allowed the measurement of NF-κB activity. Hence, co-culture of Caco-2 and THP1 cells allowed the measurement of treatments' effects on interactions between human intestinal and immune cells.

To set-up the model, Caco-2 cells were seeded in 24-well semi-permeable inserts (0.4 μm Thincerts, Greiner Bio-one, Wemmel, Belgium) at a density of 1×10^5 cells/insert. The Caco-2 cells were cultured at 37 °C in a humidified atmosphere of air/CO_2 (95:5, *v*/v) in Dulbecco's Modified Eagle Medium supplemented with heat-inactivated foetal bovine serum (HI-FBS, 20% *v*/v) and HEPES (10 mM); three medium changes were completed per week. After 14 days a functional monolayer with a transepithelial electrical resistance (TEER) of >300 Ω^*cm^2 was achieved, as measured by a Millicell ERS-2 voltohmmeter (Millipore, Massachusetts, US). Concurrently, THP1-Blue™ cells were seeded into 24-well plates at a density of 5×10^5 cells per well. Roswell Park Memorial Institute 1640 medium, supplemented with HI-FBS (10% v/v), HEPES (10 mM), and sodium pyruvate (1 mM), was used to culture the THP1-Blue™ cells at 37 °C in the same humidified environment as for the Caco-2 cells. Treatment with 50 ng/mL PMA for 48 h enabled differentiation of THP1-Blue™ cells into macrophage-like cells.

Before co-culture the TEER of an empty insert was measured; this reading was subsequently subtracted from monolayer TEER readings to account for any electrical resistance of inserts. To initiate co-culture, Caco-2 inserts were placed on top of wells containing PMA-differentiated THP1-Blue™ cells. The apical compartment, in contact with the Caco-2 monolayer, was then filled with test/control medium. For test conditions, the apical compartments were filled with luminal fluid obtained from the M-SHIME® fermentation vessels after 48 h of incubation, that had been diluted 1:5 *v*/v with Caco-2 culture medium ($n = 3$ per donor per treatment). Prior to addition, the incubation samples were sterilised *via* filtration through 0.22 μm filters to prevent microbial contamination of the cell cultures. Several control conditions were used to validate the model set-up. The first was an untreated control, whereby no further compounds were added to the apical and basolateral compartments. The second control treated the apical Caco-2 cells with 12 mM sodium butyrate. For both test and control conditions the basolateral compartment, in contact with the THP1-Blue™ monolayer, was filled with Caco-2 culture medium. After 24 h of incubation the TEER of the Caco-2 monolayers was measured and the basolateral supernatant was discarded. The basolateral compartment was then re-filled with Caco-2 culture medium containing 100 ng/mL ultrapure LPS to stimulate an inflammatory response. In a third control, the culture medium contained 100 ng/mL ultrapure LPS in combination with 1 μM hydrocortisone. After 6 h the basolateral supernatant was collected and the levels of immunoregulatory markers (IL-6, IL-8, IL-10, IL-1β, TNF-α, CXCL10, and MCP-1) were measured with the Luminex® multiplex (ThermoFisher Scientific, Massachusetts, US) according to the manufacturer instructions. NF-κB activity was determined spectrophotometrically at 690 nm as described by Possemiers et al. [48].

2.2.5. Data analysis and statistics

GraphPad Prism (Version 9.5.1) was utilised for data visualisation and statistical analysis. Differences between metabolic markers for PLGA 1, PLGA 2, and the lactate bolus for different donors at different timepoints were assessed using a two-way ANOVA with matching for each treatment across timepoints followed by a Tukey's multiple comparison test. Total BCFA synthesis was compared by summing the concentration of total BCFAs in each donor's vessels over 48 h. An ordinary one-way ANOVA was then employed to test the difference between treatments' average BCFA production across the three donors. The mean absolute and relative abundances of bacterial genera in vessels after 48 h was calculated across replicates ($n = 3$) for each donor-treatment pairing. Bray-Curtis dissimilarity was used to quantify β-diversity, and was calculated between all luminal and mucosal samples using the SciPy module (Version 1.10.1) in Python. In all cases, $P \leq 0.05$ was considered significant. Significance markers were used accordingly on plots: * $P \leq 0.05$, ** $P \leq 0.01$, *** $P \leq 0.001$, *** $P \leq 0.0001$. Unless stated otherwise, points on plots represent mean values and error bars represent standard deviation.

3. Results and discussion

3.1. Characteristics of spray dried PLGA particles

Fig. 3 shows the SEM images of the spray-dried PLGA particles tested in the M-SHIME® colon model. The spray-dried particles exhibited substantially altered morphologies and reduced sizes compared to their original forms (Fig. S2). At the micron scale, the differences between spray-dried PLGA 1 and 2 were evident. PLGA 1 particles displayed a larger size distribution than PLGA 2, with a diameter range of approximately 0.80–20 μm compared to 0.80–10 μm. PLGA 1 particles were also less spherical, displaying collapsed and occasionally hollow morphologies. Non-spherical particles have lower densities than solid particles and can be formed due to differences between polymer diffusion and solvent evaporation rates during the formation of a spray-dried particle [57]. Here, the rate of acetone evaporation during particle formation likely exceeded the rate of PLGA 1 diffusion, leading to PLGA 1 accumulation at the droplet surface and hollow particle cores susceptible to buckling [58]. PLGA 1 likely had lower diffusivity than PLGA 2 as its larger molecular weight causes stronger intermolecular interactions and more chain entanglement [59].

SEM also revealed the presence of non-spherical filaments among the PLGA 1 particles (Fig. 3A). These filaments were formed due to the rapid rate of acetone evaporation, which exceeded the rate at which droplets could be formed during atomisation of the feed solution from the spray-drying nozzle [60]. Filaments and non-spherical particles may have poorer flowability than spherical particles, potentially impacting the downstream processability of the powder during pharmaceutical manufacturing. However, it is worth noting that particles with collapsed, hollow morphologies may be more compactible (*e.g.*, for tabletting) [61]. To improve the likelihood of PLGA 1 forming spherical particles during spray drying the rate of acetone evaporation could be reduced, for example by lowering the inlet temperature and decreasing polymer concentration in the feed solution [57,60].

In contrast, PLGA 2 clearly formed smoother particles than PLGA 1, without the presence of filaments (Fig. 3B). This difference in morphology likely resulted from the lower molecular weight of PLGA 2, leading to higher polymer diffusivity and the formation of solid particles [57]. However, noticeable agglomeration was observed between PLGA 2 particles. Agglomeration likely resulted due to an increased 'stickiness' of the polymer based on its low glass transition temperature (T_g, around 30 °C) [62]. Research shows that spray drying polymers with low T_g values is challenging, as particles are more likely to stick to the spray dryer walls and agglomerate [63]. Particle stickiness is most prominent at temperatures between the T_g and 30 °C > T_g, the so-called the sticky region [64]. In this study an inlet temperature of 50 °C was used to spray dry PLGA, as per previous methods, however this temperature falls with the sticky region of PLGA 2 [65–68]. Comparatively, the T_g of PLGA 1 is

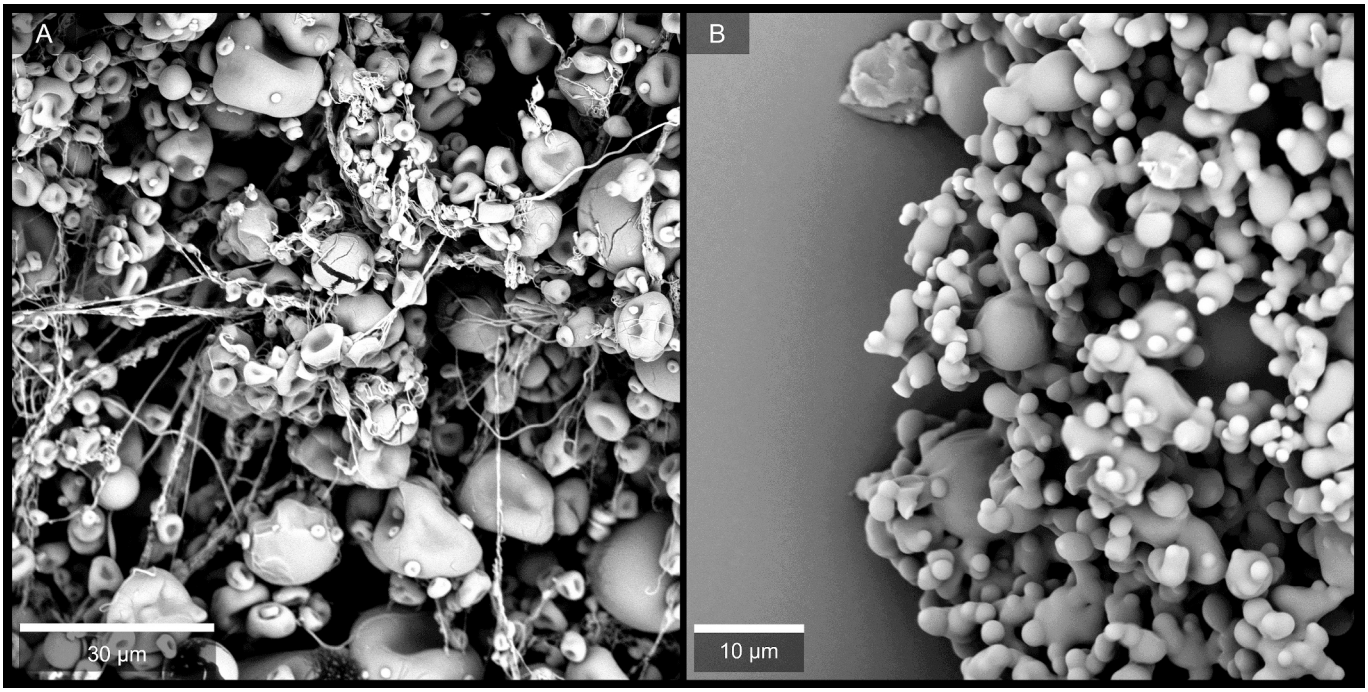

Fig. 3. Scanning electron microscopy images of the PLGA particles produced by spray drying. A: PLGA 1 (Mw 38,000–54,000 g/mol); B: PLGA 2 (Mw 2000–2500 g/mol).

46–50 °C thus its particles were less adhesive during spray drying and did not agglomerate. These findings indicate that PLGA 1 particles could have been improved by lowering inlet temperature, whilst PLGA 2 particles could have been improved by increasing the inlet temperature (above the sticky region), underscoring the complexity of spray drying and the requirement for method optimisation.

3.2. Microbiome interactions of PLGA in the M-SHIME® model of the human colon

3.2.1. Release of lactate from PLGA particles

Fig. 4 illustrates the effect of PLGA 1 and PLGA 2 particles, and the lactate bolus, on lactate concentration and pH in the M-SHIME® colonic vessels in comparison to the blank treatment-free incubations. As expected, the lactate bolus resulted in significantly higher lactate concentrations in the vessels than the blanks and the PLGA treatments (Fig. 4A). The lactate bolus was variably consumed by the microbiota from the three donors; after 48 h the microbiota from donors 1 and 2 had utilised significantly more lactate than donor 3 ($P \leq 0.0330$). It is likely that the metabolic activity of the donors' microbiota was inhibited by the lactate bolus, as the pH of cultures fell below 5.50 at several points from 6 h onwards (Fig. 4B). The lactate bolus resulted in significantly lower pH than the blank conditions for all donors at all timepoints ($P \leq 0.05$), except for donor 1 at 48 h which narrowly missed significance ($P = 0.0548$).

The lactate concentrations in the vessels dosed with PLGA 1 particles were similar to that measured in the blank (Fig. 4A). Here, lactate concentration increased in the first six hours due to microbial fermentation of fibre in the basal media and was subsequently consumed. From Fig. 4A it is clear that none of the three donors metabolised PLGA 1 to the extent that additional lactate was detectable in the vessels. In comparison, the lower molecular weight PLGA 2 provided sustained release of lactate in the presence of all three donors' microbiota (Fig. 4A). This was accompanied by a gradual decrease in pH, reaching pH 5.46–5.54 after 48 h (Fig. 4B). Lactate concentration in the vessels dosed with PLGA 2 was significantly higher than blank vessels from 0 to 48 h across donors ($P < 0.05$). In addition, the pH of vessels dosed with

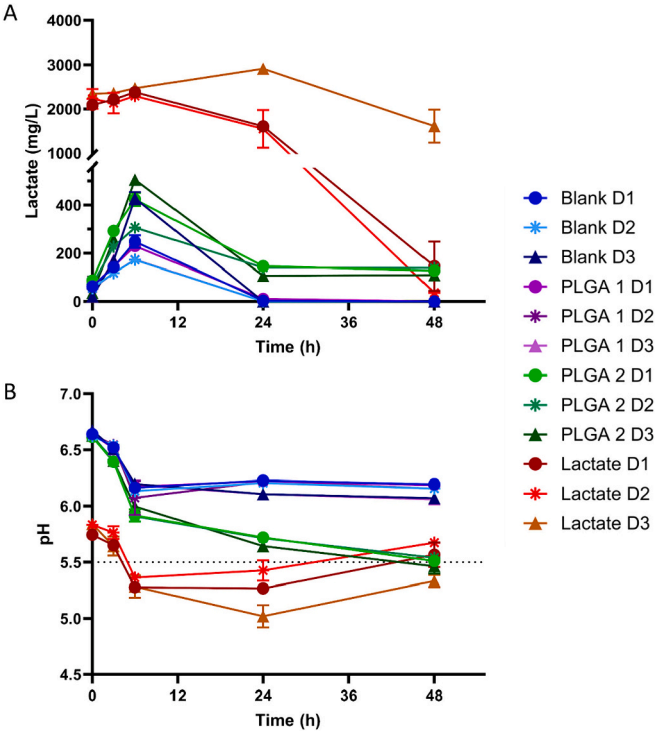

Fig. 4. A: Lactate concentration of the faecal microbiota cultures sourced from three healthy human donors, at different timepoints, when dosed at 4.5 g/L of PLGA 1 and PLGA 2, and 2.43 g/L lactic acid. B: The pH of the faecal microbiota cultures sourced from three healthy human donors, at different timepoints, when dosed at 4.5 g/L of PLGA 1 and PLGA 2, and 2.43 g/L lactic acid. The dotted line at y = 5.50 is to facilitate identification of timepoints where pH fell below a potentially toxic level for microbiota [69]. D1 - D3: donors 1–3. Measurements were conducted in triplicate and are represented as means ± SD. Significance markers are not shown due to space and instead discussed in-text.

PLGA 2 was significantly higher than those dosed with the lactate bolus from 0 to 6 h for all donors ($P \leq 0.05$) and at 24 h for donors 1 and 2 ($P \leq 0.05$), suggesting that the polymer was less toxic for the microbiota in this timeframe (Fig. 4B).

These results reveal for the first time that PLGA can be metabolised by the human gut microbiota. Whilst PLGA 1 particles were found to be stable in the presence of the microbiota, PLGA 2 particles were degraded within a surprisingly short time. This is surprising because PLGA degradation *in vivo* is reported as arising from random chain scission by water molecules over several days to months [37,70]. Whilst the present results have been captured *ex vivo*, they signify that the gut microbiota are metabolically capable of digesting PLGA, which can now be validated *in vivo*. There are several possible reasons for the different stabilities of PLGA 1 and 2. Firstly, PLGA 1's higher molecular weight would increase the number of bond scissions required for lactate liberation and could prevent bacterial ingress *via* diffusional mass transfer due to greater polymer chain entanglement. Further, PLGA 1's longer chains mean that there were fewer carboxylic end groups present to increase polymer hydrophilicity and thus enable contact with the microbiota in the aqueous incubation fluid. In addition, PLGA 1 particles had a higher maximal diameter, hence lowering the relative surface area exposed to the microbiota. The faster degradation of PLGA 2 may also have been aided by autocatalysis [71].

PLGA 1 and PLGA 2 were chosen and formulated to have the best chance of being metabolised by the gut microbiota. Compared to other marketed grades of PLGA they have low molecular weights, carboxylic acid end groups, and a 50:50 ratio of D,L-lactate to glycolate units [62]. Based on the results that PLGA 1 was not meaningfully metabolised by the microbiota, it is unlikely that higher molecular weight grades of PLGA would be metabolised either. Additionally, PLGA grades with ester, rather than carboxylic acid, end groups are also less likely to be degraded. This is because carboxylic acid groups are more hydrophilic and thus attract water molecules, leading to swelling and potentially easier enzyme access throughout the polymeric structure [70]. Further, a 50:50 ratio of D,L-lactate to glycolate provides an ideal balance for lowering T_g, achieving fully amorphous chains, and optimising the hydrophilicity of PLGA [37]. Consequently, PLGA grades with other monomeric ratios are expected to be less susceptible to microbial metabolism.

3.2.2. *Effect of PLGA on microbial metabolites and gas*

3.2.2.1. Synthesis of short chain fatty acids. Fig. 5 presents the effects of PLGA 1, PLGA 2, and the lactate bolus on the concentrations of SCFAs in the M-SHIME® colonic model compared to the blank incubations without treatment. As expected, PLGA 1 did not significantly alter acetate, propionate, or butyrate concentrations compared to the treatment-free control. These results reinforce the relative stability of the PLGA 1 particles in the medium during the observation period. In comparison, PLGA 2 showed a distinct propensity to alter SCFA synthesis. Whilst acetate production was not affected, propionate was increased in donor 3's vessels at 24 h ($P = 0.0130$) and donor 2's vessels at 48 h ($P = 0.0437$), compared to the treatment-free blanks (Fig. 5B). Furthermore, PLGA 2 significantly increased butyrate concentration in donor 1's vessels at 24 and 48 h ($P = 0.0070$ and 0.0187) and donor 2 and 3's vessels at 48 h ($P = 0.0242$ and 0.0469) (Fig. 5C). These findings indicate that the lactate released from PLGA 2 was converted to propionate and butyrate. Acetate was not increased by PLGA 2 at any of the timepoints, however may have been produced and rapidly converted to butyrate between timepoints.

In juxtaposition to PLGA, the lactate bolus exhibited clear inhibitory effects on SCFA production. Acetate concentration was reduced in donor 1's vessels at 6 and 24 h ($P \leq 0.0038$), donor 2's vessels at 3, 6, and 48 h ($P \leq 0.0395$), and donor 3's vessels at 6 and 24 h ($P \leq 0.0135$) (Fig. 5A). Propionate concentration was reduced in donor 1's vessels at 6 and 24 h

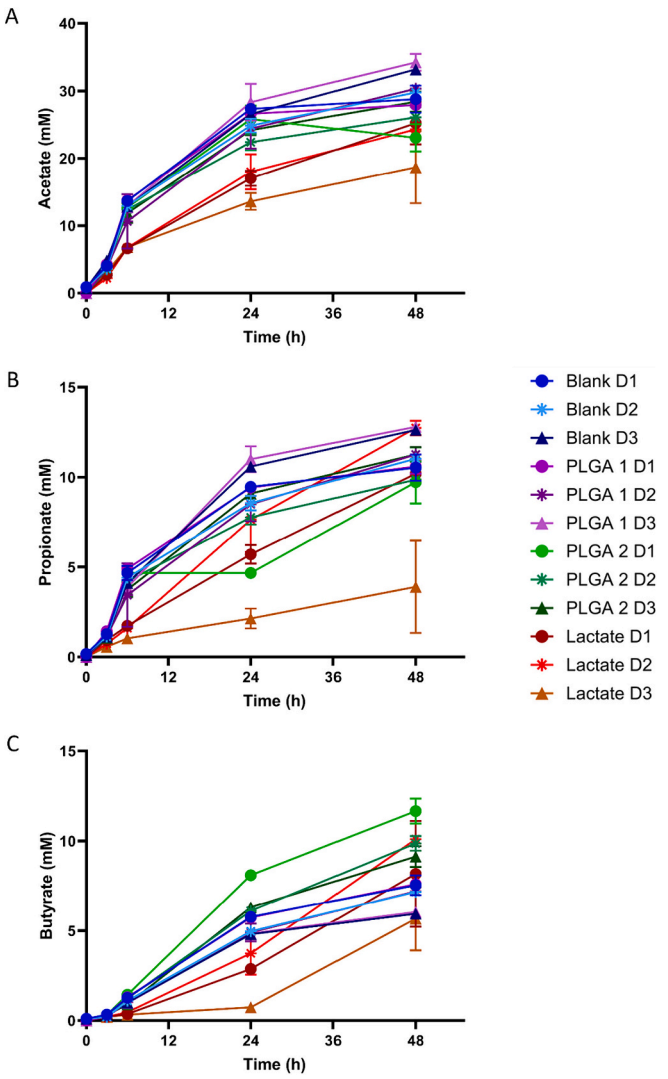

Fig. 5. The concentration of short chain fatty acids in the faecal microbiota cultures sourced from three healthy human donors, at different timepoints, when dosed at 4.5 g/L of PLGA 1 and PLGA 2, and 2.43 g/L lactic acid. Blank signifies cultures that have not been treated. A: acetate concentration; B: propionate concentration; C: butyrate concentration. D1 - D3: donors 1–3. Measurements were conducted in triplicate and are represented as means ± SD. Significance markers are not shown due to space and instead discussed in-text.

($P \leq 0.0198$), donor 2's vessels at 3 and 6 h ($P \leq 0.0129$), and donor 3's vessels at 3, 6 and 24 h ($P \leq 0.0132$) (Fig. 5B). Butyrate concentration was reduced in donor 1's vessels at 6 and 24 h ($P \leq 0.0330$) and donor 3's vessels at 3, 6 and 24 h ($P \leq 0.0141$) (Fig. 5C). However, butyrate concentration was less affected in donor 2's vessels and was even increased compared to controls at 48 h ($P = 0.0029$). These results suggest that the lactate bolus had generally toxic effects on the microbiota, with varying effects depending on the baseline microbiome composition.

3.2.2.2. Production of gas, branched chain fatty acids, and ammonium. Fig. 6 presents the effects of the interventions on gas, BCFA, and ammonium production in the M-SHIME® colonic vessels. Most gas was produced between 6 and 24 h as the microbiota multiplied and fermented the substrates in their media (Fig. 6A). After 48 h, PLGA 2 did not significantly alter gas production compared to the blank, indicating that fermentation of the polymer did not lead to significant accumulation of gases associated with SCFA synthesis, such as methane, hydrogen, and carbon dioxide [4]. Similarly, PLGA 1 and the lactate

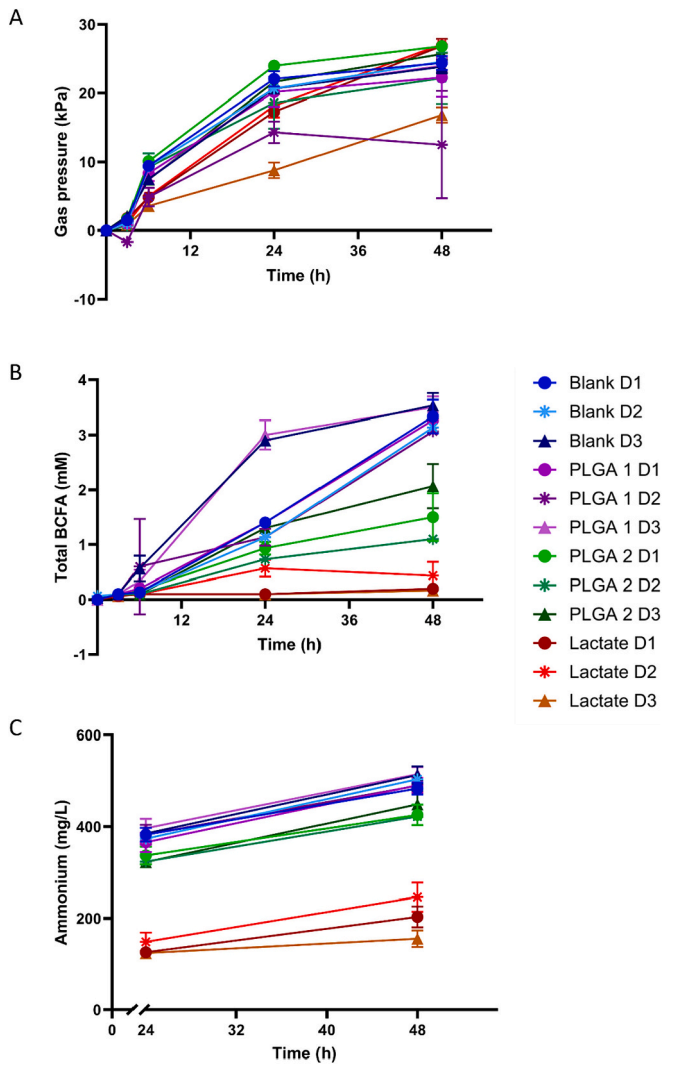

Fig. 6. The (A) gas pressure, (B) total branched chain fatty acid (BCFA), and (C) ammonium concentrations of the faecal microbiota cultures sourced from three healthy human donors, at different timepoints, when dosed at 4.5 g/L of PLGA 1 and PLGA 2, and 2.43 g/L lactic acid. Blank signifies cultures that have not been treated. D1 - D3: donors 1–3. Measurements were conducted in triplicate and are represented as means ± SD. Significance markers are not shown due to space and instead discussed in-text.

bolus also had insignificant effects on gas production, except for the lactate bolus with the donor 3 microbiota ($P = 0.0156$). The reason for the lactate bolus reducing gas output by donor 3's microbiota is likely the toxic acidification in this vessel that inhibited the samples' normal metabolic function (Fig. 4B).

Total synthesis of BCFAs was reduced across all donors by PLGA 2 and the lactate bolus ($P = 0.0261$ and 0.0018, Fig. 6B). Most BCFA synthesis occurred from 24 to 48 h, with isobutyrate and isovalerate accounting for the largest proportion of BCFAs (Fig. S3). Donor 3's microbiota produced a significantly higher concentration of valerate compared to the other two donors, demonstrating the individual nature of microbiome activity ($P < 0.0001$). BCFAs are predominately synthesised by the colonic microbiota from BCAAs during protein metabolism [72]. There is evidence that BCFAs have detrimental effects on human health [73]. For instance, faecal concentrations of isovalerate have been positively correlated with depression and cortisol levels in humans [74]. However, there is also conflicting data in the literature that BCFAs may have positive health effects in some cases [75]. Hence, drawing conclusions on PLGA's health effects *via* BCFAs may be premature, whilst research on the intestinal activities of BCFAs are further characterised [76].

As with BCFAs, ammonium concentrations were significantly reduced by the addition of PLGA 2 and the lactate bolus ($P \leq 0.0075$ at 48 h, Fig. 6C). Intestinal ammonia is generally considered to be negative for human health due to its association with neurological dysfunction, inflammation and permeability in the colonic epithelium, and promotion of colorectal cancer [77].

The microbiome's fermentation of fibre to SCFAs reduces its protein fermentation to BCFAs and associated metabolites [72]. This explains why BCFA concentrations were initially low in all vessels, as the microbiota was preferentially fermenting the fibre present in the media. Once the fibre was depleted, the microbiota in the blank and PLGA 1 vessels switched to protein metabolism, leading to increased concentrations of BCFAs and ammonium. In contrast, PLGA 2 promoted the SCFA synthesis pathway through its sustained release of lactate, resulting in reduced concentrations of BCFA and ammonium. Although the lactate bolus also reduced BCFA and ammonium concentrations this was likely due to inhibition of the microbiota's general metabolic activity as SCFA synthesis was also impaired due to the local pH-lowering effects (Figs. 4B and 5).

These findings provide evidence that controlled delivery of lactate *via* PLGA 2 could significantly elevate SCFA synthesis in the colonic environment whilst reducing ammonium and having no significant effect on gas production. Consequently, oral delivery of PLGA 2 particles to the colon could hold promise for the treatment of many diseases associated with reduced SCFA microbial synthesis [1,5–7].

3.2.3. *Effect of PLGA on microbiome composition*

3.2.3.1. Effect on the luminal microbiota. Fig. 7 illustrates the compositions of the luminal bacteria in the incubation vessels alongside the impact of the interventions on their abundance after 48 h. The full abundance results for each of the three replicates of donor-treatment pairings are available in the Supplementary Material. Each untreated luminal sample had a unique composition, which likely underpinned the differences in metabolic activity observed between donors in previous sections. Whilst these response differences are difficult to predict based on microbiome composition alone, assessment of the species present in each untreated blank sample can aid the formation of hypotheses for the samples' unique response to the treatments. For example, Actinobacteria species are known to tolerate high lactate concentrations better than *Bacteroides* species [78]. Donor 3's untreated samples had significantly lower absolute abundances of Actinobacteria ($P \leq 0.0002$) than both donor 1 and 2, and higher absolute abundances of *Bacteroides* ($P = 0.0373$) than donor 1. This may provide reasoning as to why donor 3's microbiota had relatively lower tolerance to the lactate bolus than donor 1 and donor 2's microbiota, evidenced by a greater decrease in pH and lower production of SCFAs in Figs. 4B and 5.

Compared to the blank, the lactate bolus significantly reduced absolute bacterial abundance in all donors' vessels ($P < 0.0001$). Similarly, PLGA 2 showed a significant antibacterial effect in donor 2 and 3's vessels ($P < 0.0001$); whilst PLGA 1 only reduced bacterial numbers in donor 2's vessels ($P = 0.0002$) (Fig. S4). The pronounced antibacterial effect of the lactate bolus is most likely due to its acidification of the culture media (Fig. 4B). However, the mechanism by which PLGA 1 and PLGA 2 reduced bacterial viability is less clear, particularly considering that PLGA 1 was relatively stable over the 48 h.

PLGA 2 had a positive effect on microbial activity, based on the results in Section 3.2.2. However, the results in Fig. 7 suggest that the polymer may exert negative effects on bacterial viability. As these results are based on an *in vitro* model of the colon it is essential to confirm any effect of PLGA on microbiome abundance *in vivo*. Interestingly, although the abundance of most OTUs decreased in the presence of lactate, the abundance of *Alistipes* significantly increased in donor 1's

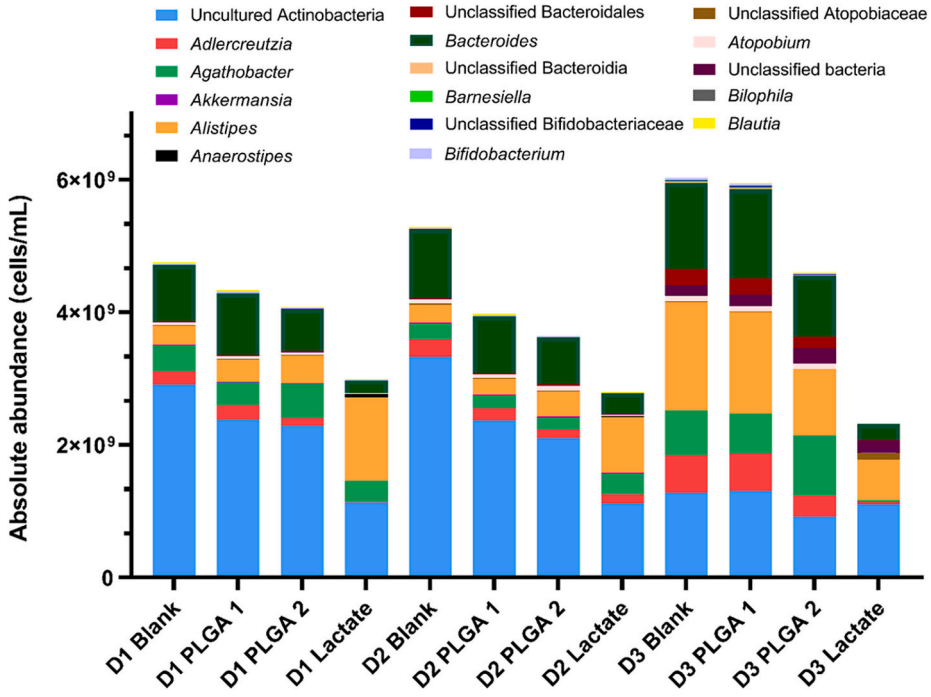

Fig. 7. The absolute abundances (cells/mL) of the 17 most common bacterial taxa in the luminal fluid of the M-SHIME® incubation vessels, 48 h after incubation with 4.5 g/L of PLGA 1 and PLGA 2, and 2.43 g/L lactic acid. Blank signifies incubation vessels that have not been treated. D1 - D3: donors 1–3. Measurements were conducted in triplicate for each donor-treatment pairing and resulting abundances are shown as mean values.

vessels ($P = 0.0011$) but not in donor 2 or 3's vessels. *Alistipes* species are known to be producers of propionate and acetate, but have also been associated with various disease states [79]. These findings highlight that the effects of the lactate bolus on microbial composition were microbiome-dependent, which aligns with the variations observed in the SCFA results (Fig. 5).

Fig. 8 presents the β-diversity of the luminal samples after 48 h. Based on the similarities of untreated blank *vs* treatment vessels, PLGA 1, PLGA 2, and the lactate bolus had a more profound impact on donor 1's microbiota than on the other two donors. Here, the lactate bolus affected donor 1's relative bacterial abundance the most (Bray-Curtis dissimilarity: 0.831), followed by PLGA 2 (Bray-Curtis dissimilarity: 0.666) and then PLGA 1 (Bray-Curtis dissimilarity: 0.545). In comparison, donor 2 and 3's microbiota was less affected by the interventions. The Bray-Curtis dissimilarities between the blank and PLGA 1, PLGA 2, and the lactate bolus for donor 2 were 0.177, 0.253, and 0.200, respectively). For donor 3 dissimilarities were even lower, at 0.105 (PLGA 1), 0.166 (PLGA 2), and 0.125 (lactate bolus). It is essential to note that the dissimilarities are based on relative rather than absolute taxonomic abundance. Therefore, though PLGA 2 reduced the number of live bacteria in donor 2 and donor 3's vessels, it did not substantially affect the proportions of taxa present. In contrast, PLGA 2 did not significantly affect bacterial viability in donor 1's vessels but did greatly alter the relative composition of bacteria. These results signify that PLGA 2 may impact both the quantity and proportions of bacteria in the colonic lumen, likely in a subject-specific manner. These *in vitro* findings underscore the need for further examination of the polymer's microbiome effects *in vivo*, involving a larger number of subjects to more comprehensively capture interindividual differences.

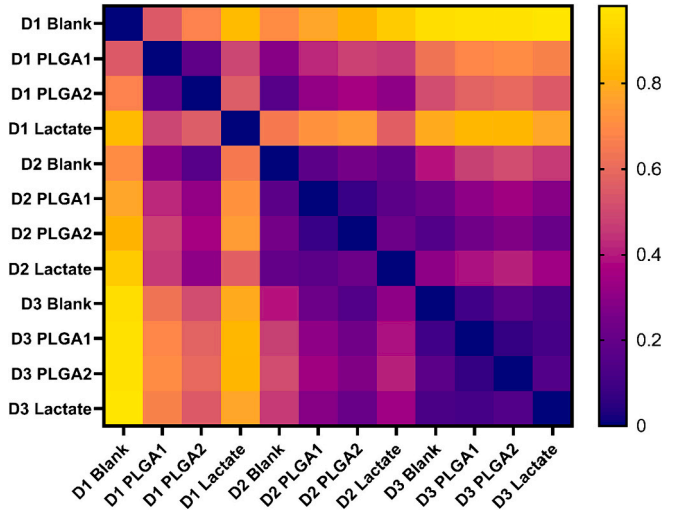

Fig. 8. The β-diversity between samples from the luminal fluid of the M-SHIME® incubation vessels, 48 h after incubation with 4.5 g/L of PLGA 1 and PLGA 2, and 2.43 g/L lactic acid. Blank signifies incubation vessels that have not been treated. β-diversity is represented as Bray-Curtis dissimilarity, which ranges from 0.00 to 1.00, where values closer to 1.00 represent higher microbiome dissimilarity. Bray-Curtis dissimilarity was calculated pairwise between all samples using the mean relative abundances of genera across three repeats. D1 - D3: donors 1–3.

3.2.3.2. Effect on the mucosal microbiota. Fig. 9 shows the effects of PLGA 1, PLGA 2, and the lactate bolus on the relative abundance of mucosal bacteria. The lactate bolus induced substantial changes in the mucosal microbiota composition in all donor's vessels. Donor 1 and 2's vessels exhibited similar alterations, with relative expansions of *Bifidobacterium, Clostridium sensu stricto*, Coriobacteriales, *Senegalimassilia*, and *Streptococcus* species. Concurrently, the abundances of *Bacteroides*, *Lachnospiraceae*, and *Roseburia* species were decreased. In donor 3's vessels the lactate bolus induced a proportional expansion of Actinobacteria, *Bifidobacterium, Clostridium sensu stricto*, *Enterococcus*, and *Lactobacillus* species, whilst increasing the abundances of almost all other species. It is likely that the sustained acidification caused by the lactate bolus selected for bacterial strains with greater tolerance to a low pH environment (Fig. 4B) [80]. For instance, several *Bifidobacterium* and

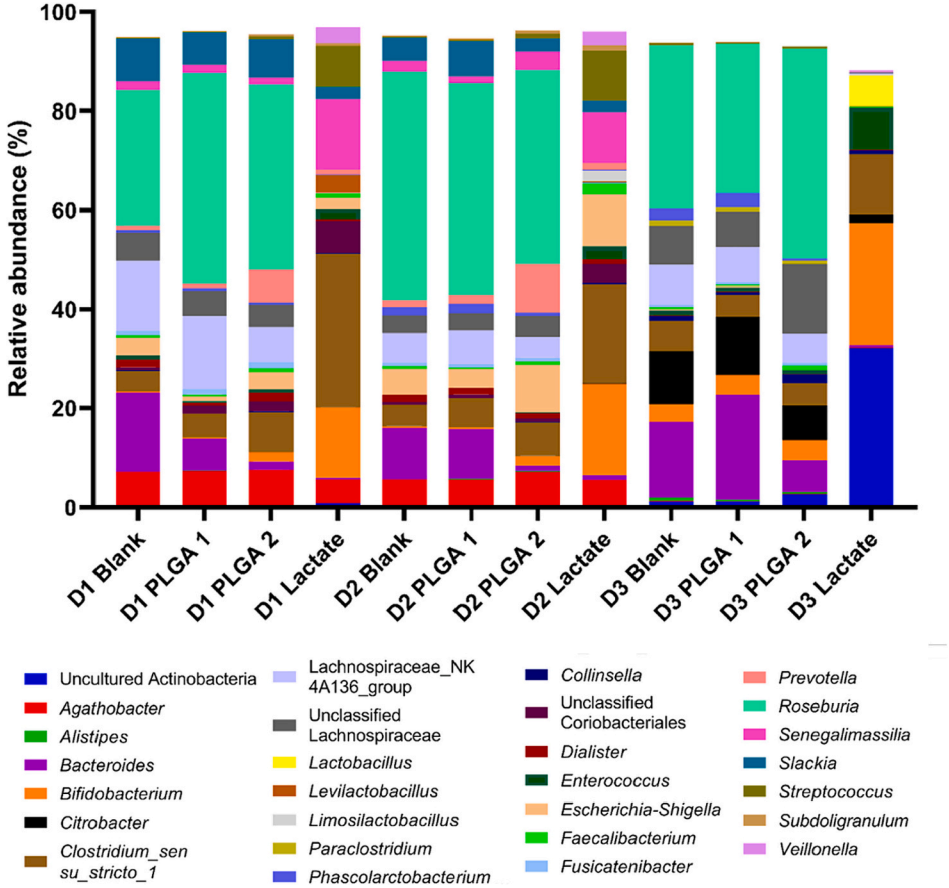

Fig. 9. The relative abundances (%) of the 28 most common bacterial taxa in the mucosal samples of the M-SHIME® incubation vessels, 48 h after incubation with 4.5 g/L of PLGA 1 and PLGA 2, and 2.43 g/L lactic acid. Blank signifies incubation vessels that have not been treated. D1 - D3: donors 1–3. Measurements were conducted in triplicate for each donor-treatment pairing and resulting abundances are shown as mean values.

Lactobacillus species have been reported to survive incubation in fluids with a pH below 5.0 [81,82]. Although some of the taxa selected by the lactate bolus are regarded as commensals (*e.g.*, *Bifidobacterium* and *Lactobacillus* species), others, such as *Clostridium sensu stricto*, *Streptococcus,* and *Enterococcus* species, have been associated with pathogenic properties [83,84]. The combination of these findings with the metabolite data suggests that the lactate bolus shifted the mucosal microbiota towards a more dysbiotic state.

Compared to the lactate bolus, PLGA 2 had a lower impact on donor 1's mucosal bacteria (Fig. 9). This is reflected in a lower β-diversity between PLGA 2 and donor 1's blank compared to the lactate bolus and donor 1's blank (Bray-Curtis dissimilarity 0.703 *vs* 0.860) (Fig. 10). The β-diversities between PLGA 2 and donor 2 and 3's blanks (donor 2: 0.267; donor 3: 0.181) were similar to those between the lactate bolus and donor 2 and 3's blanks (donor 2: 0.224; donor 3: 0.141). Hence, PLGA 2 altered the bacterial composition of donor 2 and 3's microbiota to a quantitatively similar extent as the lactate bolus. These results underscore the importance of qualitatively and quantitatively analysing microbiome data, as the results in Fig. 9 suggest that PLGA 2 had a less profound impact on microbiome composition than lactate.

PLGA 2 significantly reduced the proportion of *Bacteroides* in donor 1's vessels ($P = 0.006$). Generally, the β-diversity results show that donor 1's microbiota was the most sensitive to alterations by the interventions. However, PLGA 2 also significantly increased the relative abundance of *Prevotella* species in donor 2's vessels ($P = 0.0298$). This relative increase in *Bacteroides* species in donor 1's vessels and decrease in *Prevotella* species in donor 2's vessels is interesting, as these two genera have been associated with human lifestyle and health [85]. High *Bacteroides* and low *Prevotella* abundance has been associated with the Western diet,

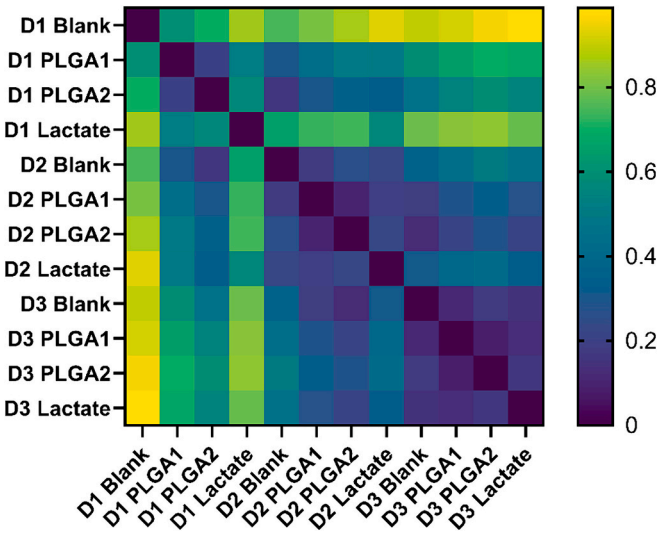

Fig. 10. The β-diversity between samples from the mucosal beads of the M-SHIME® incubation vessels, 48 h after incubation with 4.5 g/L of PLGA 1 and PLGA 2, and 2.43 g/L lactic acid. Blank signifies incubation vessels that have not been treated. β-diversity is represented as Bray-Curtis dissimilarity, which ranges from 0.00 to 1.00, where values closer to 1.00 represent higher microbiome dissimilarity. Bray-Curtis dissimilarity was calculated pairwise between all samples using the mean relative abundances of genera across three repeats. D1 - D3: donors 1–3.

which is high in protein, fat, and ultra-processed foods [86]. Conversely, high *Prevotella* and low *Bacteroides* abundance has been associated with plant-based diets rich in polysaccharides [87]. The increase in *Prevotella* abundance in donor 2's vessels may be explained by *Prevotella* species' high expression of carbohydrate metabolising enzymes (CAZy). The fermentation of PLGA 2 by bacterial CAZy, such as esterases, could have thus selected for *Prevotella* species [87]. These results provide early evidence that PLGA 2 may promote a favourable shift in the mucosal microbiome, away from compositions associated with the Western diet and disease [88]. However, to validate these findings, further investigations should be conducted *in vivo*, involving multiple individuals and longer durations of PLGA 2 administration. Such studies will offer more robust insights into the impact of PLGA 2 on microbiome composition and its potential as a beneficial therapeutic approach.

3.3. Effect of PLGA on an IBD-like intestinal epithelium

3.3.1. Effect on epithelial integrity

Fig. 11 illustrates the effect of the interventions on the integrity of a Caco-2 monolayer in contact with macrophage-like THP1-Blue™ cells. As expected, the sodium butyrate control significantly protected the Caco-2 monolayer from damage induced by the THP1-Blue™ cells (Fig. S5). Luminal samples taken from donor 1's vessels maintained Caco-2 integrity, independent of the treatment administered to vessels. This suggests that donor 1's microbiota conferred inherent protection against epithelial damage that was not improved by PLGA 1, PLGA 2, or the lactate bolus.

In the case of donor 2, the blank and PLGA 1 samples led to a reduction in TEER of the Caco-2 cells due to THP1-Blue™ cell-induced damage (Fig. 11). However, fluid from donor 2's PLGA 2 and the lactate bolus vessels significantly protected the integrity of the Caco-2 monolayer. Notably, donor 2's PLGA 2 and lactate bolus vessels contained significantly lower ammonium levels compared to the blank and PLGA 1 vessels (Fig. 6C). In addition, PLGA 2 increased propionate and butyrate concentrations in donor 2's vessels, and the lactate bolus increased final butyrate concentrations (Fig. 5). These results suggest that PLGA 2 and the lactate bolus may have provided protection to the Caco-2 cells by reducing the concentration of pro-inflammatory ammonium (both treatments), and increasing concentrations of anti-inflammatory SCFAs in the fluids (for PLGA 2, only).

In the case of donor 3, the blank and PLGA 1 fluids also did not protect the Caco-2 monolayer. Although samples from donor 3's PLGA 2 vessels numerically increased TEER compared to the blank, this increase narrowly missed statistical significance ($P = 0.0589$). However, samples from donor 3's lactate bolus vessels did significantly protect the integrity of the cells ($P = 0.0103$). Notably, the lactate bolus exerted a generally toxic effect on donor 3's microbiota, leading to a sustained decrease in pH (Fig. 4B), reduced synthesis of SCFAs (Fig. 5), and decreased absolute abundance of luminal bacteria (Fig. 7). This inhibitory action on microbiota also reduced the synthesis of pro-inflammatory ammonium, potentially explaining the observed protective effects on Caco-2 TEER.

3.3.2. Effect on anti-inflammatory IL-10

Fig. 12 depicts the impact of treatments on the anti-inflammatory cytokine IL-10 in the basolateral compartment of the Caco-2/THP1 co-culture model. As expected, the positive control, hydrocortisone, significantly increased IL-10 secretion (Fig. S6C), confirming the validity of the assay. PLGA 1 had no effect on IL-10 secretion for any donor, and PLGA 2 and the lactate bolus were only significant for one donor each. Incubation fluids treated with PLGA 2 promoted a statistically significant increase in IL-10 secretion from cells for samples taken from donor 1's vessels ($P = 0.0316$). In this case, but not for donor 2 and 3, PLGA 2 showed anti-inflammatory potential. In contrast, donor 3's fluids treated with the lactate bolus had a negative impact on IL-10 secretion. Whilst this is also limited to one donor, and thus broad conclusions cannot be made, it signifies that the lactate bolus was potentially pro-inflammatory in this situation. Overall, none of the treatments had a clear impact on IL-10 as the three donors were not uniformly affected.

3.3.3. Effect on pro-inflammatory markers

Fig. 13 presents the impact of treatments on pro-inflammatory markers in the basolateral compartment of the Caco-2/THP1 co-culture model. These markers, including cytokines (IL-6, IL-8, IL-1β, TNF-α), chemokines (CXCL10, MCP-1), and a transcription factor (NF-κB), are known to be positively associated with inflammation, with higher concentrations indicating a greater degree of pro-inflammatory signalling [89–95]. The results from the controls were in line with that expected (Fig. S6).

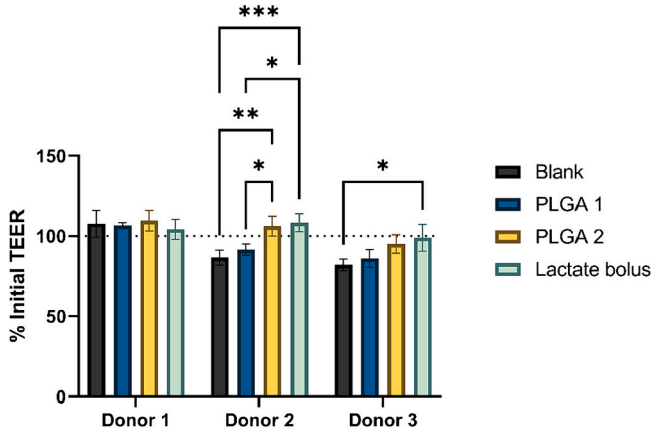

Fig. 11. The effect of treatments on the transepithelial electrical resistance (TEER, Ω*cm^2) of Caco-2 monolayers. Results are presented as the TEER 24 h following treatment with diluted fluid obtained from the M-SHIME® fermentation vessels after 48 h of incubation, as a percentage of initial TEER at time zero (100%, represented by the dotted line). Blank: untreated M-SHIME® vessels; PLGA 1: vessels treated with 4.5 g/L PLGA 1 particles; PLGA 2: vessels treated with 4.5 g/L PLGA 2 particles; lactate bolus: vessels treated with 2.43 g/L lactic acid. The mean TEER value for the epithelial model at 0 h, across donors and treatments, was 1462 ± 151 Ω*cm^2. $N = 3$ for each donor-treatment pairing, with results represented as means ± SD.

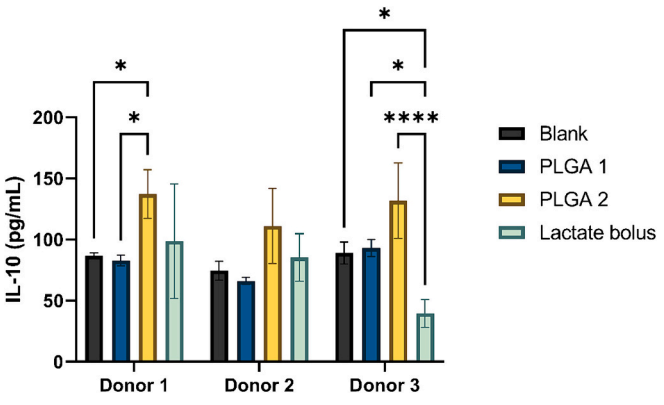

Fig. 12. The effect of treatments on IL-10 concentration in the basolateral supernatant of the Caco-2/THP1 co-culture model. IL-10 was measured 6 h after basolateral lipopolysaccharide stimulation of the Caco-2/THP1-Blue™ co-cultures following apical pre-treatment for 24 h with fluid from M-SHIME® incubation vessels that had been diluted 1:5 *v*/v with Caco-2 culture medium. Blank: untreated M-SHIME® vessels; PLGA 1: vessels treated with 4.5 g/L PLGA 1 particles; PLGA 2: vessels treated with 4.5 g/L PLGA 2 particles; lactate bolus: vessels treated with 2.43 g/L lactic acid. $N = 3$ for each donor-treatment pairing with results represented as means ± SD. (For interpretation of the references to colour in this figure legend, the reader is referred to the web version of this article.)

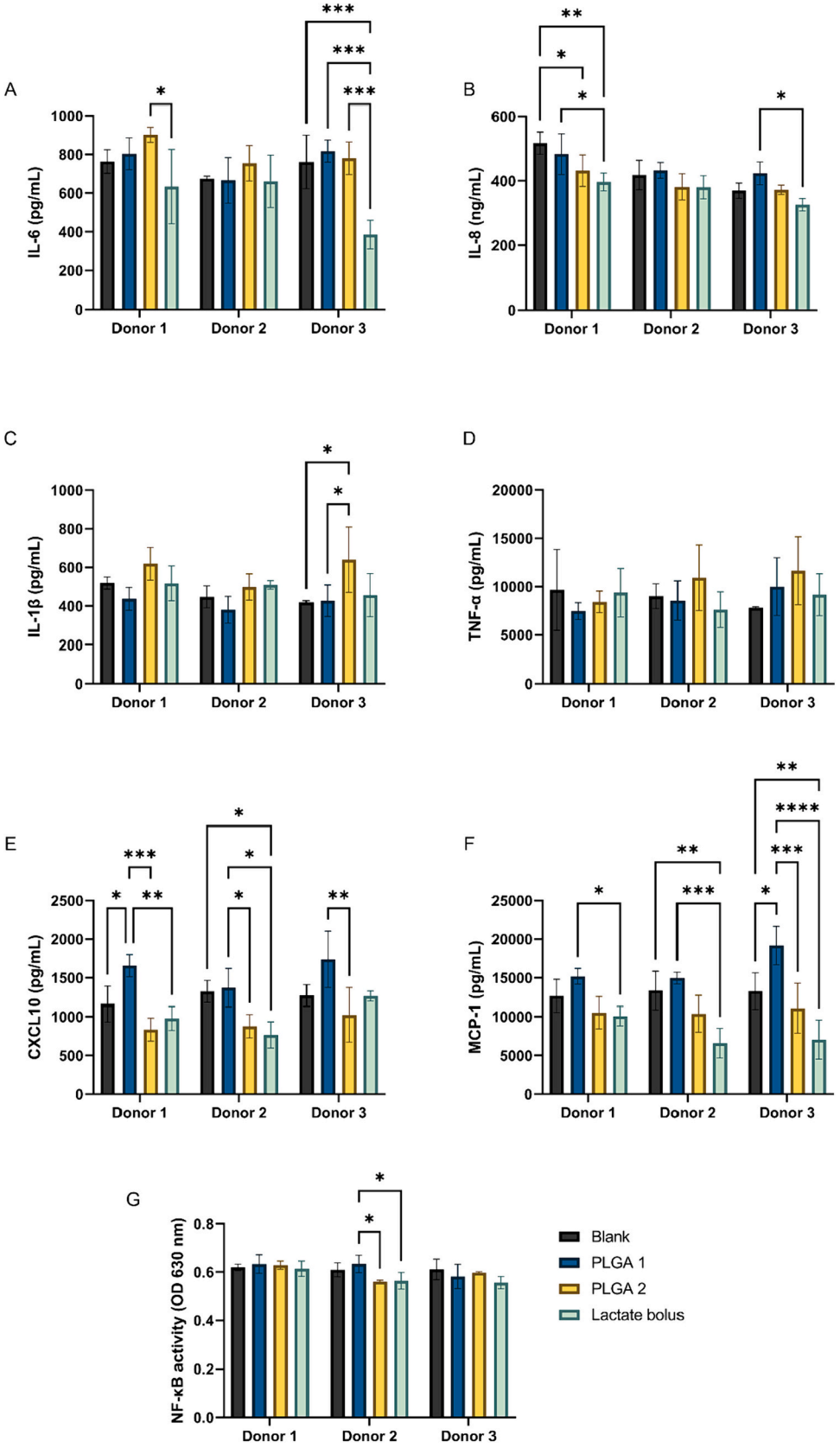

Fig. 13. The effect of treatments on pro-inflammatory markers present in the basolateral supernatant of the Caco-2/THP1 co-culture model. Markers were measured 6 h after basolateral lipopolysaccharide stimulation of the Caco-2/THP1-Blue™ co-cultures following apical pre-treatment for 24 h with fluid from M-SHIME® incubation vessels that had been diluted 1:5 v/v with Caco-2 culture medium. Blank: untreated M-SHIME® vessels; PLGA 1: vessels treated with 4.5 g/L PLGA 1 particles; PLGA 2: vessels treated with 4.5 g/L PLGA 2 particles; lactate bolus: vessels treated with 2.43 g/L lactic acid. $N = 3$ for each donor-treatment pairing with results represented as means ± SD. (For interpretation of the references to colour in this figure legend, the reader is referred to the web version of this article.)

PLGA 2 fluids demonstrated mostly neutral activity in the cell model. The polymer had no significant effect on IL-6, TNF-α, CXCL10, or MCP-1 concentrations compared to the blank. However, in one instance PLGA 2 exhibited anti-inflammatory action: donor 1's fluids treated with PLGA 2 showed significantly lower concentrations of IL-8 ($P = 0.0430$) than the blank. Furthermore, in several cases PLGA 2 displayed less pro-inflammatory potential than PLGA 1, evidenced by reduced CXCL10 concentrations in samples from all donor fluids ($P < 0.05$), MCP-1 concentrations in samples from donor 3 ($P = 0.0007$), and NF-κB in samples from donor 2 ($P = 0.0360$).

In two cases PLGA 1 was more inflammatory than the blank: CXCL10 concentrations in samples from donor 1 ($P = 0.0446$), and MCP-1 concentrations in samples from donor 3 ($P = 0.0136$). PLGA 2 was found to be more inflammatory than the blank in one instance, where donor 3 fluids treated with PLGA 2 provoked secretion of IL-1β ($P = 0.0150$).

PLGA 1 had neutral effects on cytokines, but its stimulation of the CXCL10 and MCP-1 chemokines is intriguing. *In vivo*, these chemokines play a role in leukocyte recruitment, and have been associated with greater disease severity in IBD [96,97]. While PLGA is generally regarded as fully biocompatible, and included in various marketed formulations, it is essential to consider the potential pro-inflammatory properties of its molecular cousin, PLA [98]. A recent study showed that PLA oligomers can cause acute intestinal and hepatic inflammation in mice by binding to matrix metallopeptidase 12 (MMP12), leading to significantly increased TNF-α. PLA oligomers bind to MMP12 *via* electrostatic interactions between PLA's carboxyl groups and MMP12's zinc ions. Though PLGA has a similar structure to PLA, it may have insignificant affinity for MMP12 due to the larger space between its carboxyl groups. Further, neither PLGA treatments were found to affect TNF-α in the cell culture model.

3.4. Translational potential of PLGA

It is envisaged that PLGA 2 would be formulated for oral administration, and would transit through the GI tract before being metabolised by the colonic microbiota to provide sustained lactate release. It is not expected that PLGA 2 would be significantly degraded in the stomach or small intestine, as these regions have substantially lower microbial abundances than the colon [99]. However, if upper GI degradation of PLGA 2 was identified as a challenge, then the polymer could be formulated for colon-specific release [54]. PLGA 2 offers several advantages over existing products designed to increase colonic SCFA concentrations. Firstly, it is considerably less challenging to work with than probiotics, which often experience reduced efficacy due to inactivation during formulation and transit through the GI tract [34]. Secondly, precise dosing is achievable with PLGA whereas quantifying the exact number and activity of live bacteria within probiotic products is difficult and can vary between batches. Thirdly, at an effective concentration of 4.5 g/L and an estimated colonic fluid volume of 560 mL, human adults would require a PLGA 2 dose of around 2.50 g, which is significantly less than that required for prebiotics [54]. As such, PLGA 2 is expected to be less burdensome for patients in terms of administration and may achieve higher compliance compared to prebiotics.

With all results, it is important to keep in mind the limitations of the models used. The M-SHIME® and epithelial cell models are *ex vivo/in vitro* techniques, thus data may not fully reflect *in vivo* outcomes. In addition, these results are based on the microbiota sourced from three healthy donors, and outcomes may vary when assessing a larger population and/or individuals with disease. The results in this study outline that PLGA 2 can be degraded by the gut microbiota, which could be leveraged for sustained delivery of lactate over the course of colonic transit. The extent to which SCFA synthesis is increased, microbiome composition is altered, and epithelial function is modulated will be best characterised *in vivo*; however, the present data provide a useful foundation for planning and justifying *in vivo* experiments. An avenue for future investigation could be the estimation of an ideal rate of lactate release from the PLGA particles, to enable optimal stimulation of SCFA production in the colon.

Though the positive findings for PLGA 2 administration outnumbered the negative, it is important to highlight the data that was not in full support of the polymer. Namely, PLGA 2 reduced the number of live bacteria in the luminal incubation samples. This raises concerns that the polymer could reduce bacterial viability *in vivo*. Additionally, one donor's luminal fluids incubated with the polymer increased concentrations of pro-inflammatory IL-1β in the epithelial cell culture model. Further, several effects of PLGA 2 were observed in a donor-dependent manner, suggesting the significance of individual microbiome compositions for response to PLGA 2 treatment, which could lead to inter- and/or intra-individual variability in the clinic. As PLGA 2 is progressed to *in vivo* studies, it is advised that analyses investigate both favourable and unfavourable consequences of PLGA 2 administration. This will enable proper appraisal of the product's potential as a novel microbiome medicine.

4. Conclusions

This study investigated PLGA nano-microparticles as a means of increasing microbial synthesis of SCFAs in the colon. The results showed that PLGA particles with a molecular weight of 2000–2500 g/mol (PLGA 2), but not 38,000–54,000 g/mol (PLGA 1), were significantly degraded by the human faecal microbiota in the short-term colon M-SHIME® system. PLGA 2 metabolism led to sustained release of lactate in the presence of all donors' microbiota over 48 h, with milder effects on cultures' pH compared to a lactate bolus. PLGA 2 significantly increased microbial synthesis of butyrate in all donors' vessels, in addition to reducing the production of harmful ammonium. The PLGA 2 particles had a mainly neutral effect on the *in vitro* model of the intestinal epithelium, leading to minor and donor-specific changes in epithelial integrity and inflammatory marker expression. PLGA 2 was also found to alter luminal and mucosal microbiome composition in all donors' vessels. Here, effects on relative abundances were generally deemed as neutral or beneficial, whilst the absolute abundance of luminal bacteria was significantly reduced in two donors' cultures. In conclusion, this study revealed the susceptibility of PLGA to metabolism by human faecal microbiota, a trait that could be exploited to increase concentrations of SCFAs in the colon. Onward investigation will focus on optimising the formulation of PLGA for colonic delivery, leading to its assessment as a microbiome therapeutic *in vivo*.

CRediT authorship contribution statement

Laura E. McCoubrey: Writing – review & editing, Writing – original draft, Visualization, Project administration, Methodology, Investigation, Formal analysis, Data curation, Conceptualization. **Fabiana Ferraro:** Methodology, Investigation, Formal analysis, Data curation. **Nidhi Seegobin:** Writing – review & editing, Methodology, Investigation, Data curation. **Jérémy Verin:** Investigation. **Haya A. Alfassam:** Investigation. **Atheer Awad:** Writing – review & editing, Visualization, Project administration. **Massimo Marzorati:** Resources, Investigation. **Lynn Verstrepen:** Investigation, Formal analysis, Data curation. **Jonas Ghyselinck:** Methodology, Investigation, Formal analysis, Data curation. **Julie De Munck:** Investigation, Formal analysis, Data curation. **Jelle De Medts:** Investigation, Formal analysis, Data curation. **Evi Steppe:** Investigation, Formal analysis, Data curation. **Valerie De Vleeschhauwer:** Investigation, Formal analysis, Data curation. **Gilles De Rocker:** Investigation, Formal analysis, Data curation. **Alexandra Droesbeke:** Investigation, Formal analysis, Data curation. **Melanie De Rijck:** Investigation, Formal analysis, Data curation. **Sara Vanthoor:** Investigation, Formal analysis, Data curation. **Frédéric Moens:** Writing – review & editing, Project administration, Investigation, Funding acquisition, Formal analysis, Data curation. **Juergen Siepmann:** Writing – review & editing, Supervision, Resources, Project

administration, Methodology, Funding acquisition. **Florence Siepmann:** Writing – review & editing, Supervision, Resources, Project administration, Methodology, Funding acquisition. **Simon Gaisford:** Supervision, Conceptualization. **Mine Orlu:** Supervision. **Abdul W. Basit:** Writing – review & editing, Supervision, Resources, Project administration, Methodology, Funding acquisition, Conceptualization.

Declaration of competing interest

None.

Data availability

Data will be made available on request.

Acknowledgements

The valuable feedback from Dr. David Shorthouse and Prof. Ben Forbes on this work was highly appreciated. The authors acknowledge The Engineering and Physical Sciences Research Council [grant EP/S023054/1] to UCL School of Pharmacy, and The Interreg 2 Seas programme 2014–2020 co-funded by the European Regional Development Fund under subsidy contract "Site Drug 2S07-033", for funding this work.

Appendix A. Supplementary data

Supplementary data to this article can be found online at https://doi.org/10.1016/j.jconrel.2024.03.039.

References

[1] J.L. McCarville, G.Y. Chen, V.D. Cuevas, K. Troha, J.S. Ayres, Microbiota metabolites in health and disease, Annu. Rev. Immunol. 38 (2020) 147–170.
[2] V. Rothhammer, F.J. Quintana, The aryl hydrocarbon receptor: an environmental sensor integrating immune responses in health and disease, Nat. Rev. Immunol. 19 (2019) 184–197.
[3] A. Rutsch, J.B. Kantsjo, F. Ronchi, The gut-brain axis: how microbiota and host inflammasome influence brain physiology and pathology, Front. Immunol. 11 (2020) 604179.
[4] D. Parada Venegas, M.K. De la Fuente, G. Landskron, M.J. Gonzalez, R. Quera, G. Dijkstra, H.J.M. Harmsen, K.N. Faber, M.A. Hermoso, Short chain fatty acids (SCFAs)-mediated gut epithelial and immune regulation and its relevance for inflammatory bowel diseases, Front. Immunol. 10 (2019) 277.
[5] L. Zhao, F. Zhang, X. Ding, G. Wu, Y.Y. Lam, X. Wang, H. Fu, X. Xue, C. Lu, J. Ma, L. Yu, C. Xu, Z. Ren, Y. Xu, S. Xu, H. Shen, X. Zhu, Y. Shi, Q. Shen, W. Dong, R. Liu, Y. Ling, Y. Zeng, X. Wang, Q. Zhang, J. Wang, L. Wang, Y. Wu, B. Zeng, H. Wei, M. Zhang, Y. Peng, C. Zhang, Gut bacteria selectively promoted by dietary fibers alleviate type 2 diabetes, Science 359 (2018) 1151.
[6] R. Corrêa-Oliveira, J.L. Fachi, A. Vieira, F.T. Sato, M.A.R. Vinolo, Regulation of immune cell function by short-chain fatty acids, Clin. Transl. Immunol. 5 (2016) e73.
[7] A.N. Thorburn, C.I. McKenzie, S. Shen, D. Stanley, L. Macia, L.J. Mason, L. K. Roberts, C.H.Y. Wong, R. Shim, R. Robert, N. Chevalier, J.K. Tan, E. Mariño, R. J. Moore, L. Wong, M.J. McConville, D.L. Tull, L.G. Wood, V.E. Murphy, J. Mattes, P.G. Gibson, C.R. Mackay, Evidence that asthma is a developmental origin disease influenced by maternal diet and bacterial metabolites, Nat. Commun. 6 (2015) 7320.
[8] E.R. Hutchison, K. Kasahara, Q. Zhang, E.I. Vivas, T.L. Cross, F.E. Rey, Dissecting the impact of dietary fiber type on atherosclerosis in mice colonized with different gut microbial communities, NPJ Biofilms Microbiom. 9 (2023) 31.
[9] X. Ye, H. Li, K. Anjum, X. Zhong, S. Miao, G. Zheng, W. Liu, L. Li, Dual role of indoles derived from intestinal microbiota on human health, Front. Immunol. 13 (2022) 903526.
[10] K.N. Prasad, A. Sakamoto, Effect of sodium butyrate in combination with prostaglandin E1 and inhibitors of cyclic nucleotide phosphodiesterase on human amelanotic melanoma cells in culture, Experientia 34 (1978) 1575–1576.
[11] P.R. Pouillart, Role of butyric acid and its derivatives in the treatment of colorectal cancer and hemoglobinopathies, Life Sci. 63 (1998) 1739–1760.
[12] K.N. Prasad, Butyric acid: a small fatty acid with diverse biological functions, Life Sci. 27 (1980) 1351–1358.
[13] S. Facchin, N. Vitulo, M. Calgaro, A. Buda, C. Romualdi, D. Pohl, B. Perini, G. Lorenzon, C. Marinelli, R. D'Incà, G.C. Sturniolo, E.V. Savarino, Microbiota changes induced by microencapsulated sodium butyrate in patients with inflammatory bowel disease, Neurogastroenterol. Motil. 32 (2020) e13914.
[14] M.A.G. Hernandez, E.E. Canfora, J.W.E. Jocken, E.E. Blaak, The short-chain fatty acid acetate in body weight control and insulin sensitivity, Nutrients 11 (2019).
[15] P.A. Gill, M.C. van Zelm, J.G. Muir, P.R. Gibson, Review article: short chain fatty acids as potential therapeutic agents in human gastrointestinal and inflammatory disorders, Aliment. Pharmacol. Ther. 48 (2018) 15–34.
[16] X. Zhu, C. Jia, X. Meng, M. Xing, Y. Yi, X. Gao, Synthesis, characterization of inulin propionate ester, and evaluation of its in vitro effect on SCFA production, Starch - Stärke 70 (2018) 1800037.
[17] E.S. Chambers, A. Viardot, A. Psichas, D.J. Morrison, K.G. Murphy, S.E.K. Zac-Varghese, K. MacDougall, T. Preston, C. Tedford, G.S. Finlayson, J.E. Blundell, J. D. Bell, E.L. Thomas, S. Mt-Isa, D. Ashby, G.R. Gibson, S. Kolida, W.S. Dhillo, S. R. Bloom, W. Morley, S. Clegg, G. Frost, Effects of targeted delivery of propionate to the human colon on appetite regulation, body weight maintenance and adiposity in overweight adults, Gut 64 (2015) 1744–1754.
[18] E.S. Chambers, C.S. Byrne, A. Rugyendo, D.J. Morrison, T. Preston, C. Tedford, J. D. Bell, L. Thomas, A.N. Akbar, N.E. Riddell, R. Sharma, M.R. Thursz, P. Manousou, G. Frost, The effects of dietary supplementation with inulin and inulin-propionate ester on hepatic steatosis in adults with non-alcoholic fatty liver disease, Diabetes Obes. Metab. 21 (2019) 372–376.
[19] T. Polyviou, K. MacDougall, E.S. Chambers, A. Viardot, A. Psichas, S. Jawaid, H. C. Harris, C.A. Edwards, L. Simpson, K.G. Murphy, S.E.K. Zac-Varghese, J. E. Blundell, W.S. Dhillo, S.R. Bloom, G.S. Frost, T. Preston, M.C. Tedford, D. J. Morrison, Randomised clinical study: inulin short-chain fatty acid esters for targeted delivery of short-chain fatty acids to the human colon, Aliment. Pharmacol. Ther. 44 (2016) 662–672.
[20] C.M. Holman, T. Minssen, E.M. Solovy, Patentability standards for follow-on pharmaceutical innovation, Biotechnol. Law Rep. 37 (2018) 131–161.
[21] F. Moens, P. Van den Abbeele, A.W. Basit, C. Dodoo, R. Chatterjee, B. Smith, S. Gaisford, A four-strain probiotic exerts positive immunomodulatory effects by enhancing colonic butyrate production in vitro, Int. J. Pharm. 555 (2019) 1–10.
[22] A. Ferreira-Lazarte, F.J. Moreno, C. Cueva, I. Gil-Sánchez, M. Villamiel, Behaviour of citrus pectin during its gastrointestinal digestion and fermentation in a dynamic simulator (simgi®), Carbohydr. Polym. 207 (2019) 382–390.
[23] S. Serrano-Villar, J.F. Vázquez-Castellanos, A. Vallejo, A. Latorre, T. Sainz, S. Ferrando-Martínez, D. Rojo, J. Martínez-Botas, J. del Romero, N. Madrid, M. Leal, J.I. Mosele, M.J. Motilva, C. Barbas, M. Ferrer, A. Moya, S. Moreno, M. J. Gosalbes, V. Estrada, The effects of prebiotics on microbial dysbiosis, butyrate production and immunity in HIV-infected subjects, Mucosal Immunol. 10 (2017) 1279–1293.
[24] A. Vijay, S. Astbury, C. Le Roy, T.D. Spector, A.M. Valdes, The prebiotic effects of omega-3 fatty acid supplementation: a six-week randomised intervention trial, Gut Microbes 13 (2021) 1–11.
[25] D. Davani-Davari, M. Negahdaripour, I. Karimzadeh, M. Seifan, M. Mohkam, S. J. Masoumi, A. Berenjian, Y. Ghasemi, Prebiotics: definition, types, sources, mechanisms, and clinical applications, Foods 8 (2019) 92.
[26] K. Kailasapathy, J. Chin, Survival and therapeutic potential of probiotic organisms with reference to *Lactobacillus acidophilus* and *Bifidobacterium* spp, Immunol. Cell Biol. 78 (2000) 80–88.
[27] R.L.J. Day, A.J. Harper, R.M. Woods, O.G. Davies, L.M. Heaney, Probiotics: current landscape and future horizons, Future Sci. OA 5 (2019).
[28] S.L. Hudson, G. Arnoczy, H. Gibson, C. Thurber, J. Lee, A. Kessell, Probiotic use as prophylaxis for *Clostridium difficile*-associated diarrhea in a community hospital, Am. J. Infect. Control 47 (2019) 1028–1029.
[29] C. Tenorio-Jimenez, M.J. Martinez-Ramirez, A. Gil, C. Gomez-Llorente, Effects of probiotics on metabolic syndrome: a systematic review of randomized clinical trials, Nutrients 12 (2020).
[30] M. Yao, Y. Lu, T. Zhang, J. Xie, S. Han, S. Zhang, Y. Fei, Z. Ling, J. Wu, Y. Hu, S. Ji, H. Chen, B. Berglund, L. Li, Improved functionality of *Ligilactobacillus salivarius* Li01 in alleviating colonic inflammation by layer-by-layer microencapsulation, NPJ Biofilms Microbiom. 7 (2021) 58.
[31] Y. Yu, S. Dunaway, J. Champer, J. Kim, A. Alikhan, Changing our microbiome: probiotics in dermatology, Br. J. Dermatol. 182 (2020) 39–46.
[32] M. Cunningham, M.A. Azcarate-Peril, A. Barnard, V. Benoit, R. Grimaldi, D. Guyonnet, H.D. Holscher, K. Hunter, S. Manurung, D. Obis, M.I. Petrova, R. E. Steinert, K.S. Swanson, D. van Sinderen, J. Vulevic, G.R. Gibson, Shaping the future of probiotics and prebiotics, Trends Microbiol 29 (2021) 667–685.
[33] S. Klayraung, H. Viernstein, S. Okonogi, Development of tablets containing probiotics: effects of formulation and processing parameters on bacterial viability, Int. J. Pharm. 370 (2009) 54–60.
[34] M. Fredua-Agyeman, S. Gaisford, Comparative survival of commercial probiotic formulations: tests in biorelevant gastric fluids and real-time measurements using microcalorimetry, Benefic. Microbes 6 (2015) 141–151.
[35] J. Suez, N. Zmora, E. Segal, E. Elinav, The pros, cons, and many unknowns of probiotics, Nat. Med. 25 (2019) 716–729.
[36] P. Louis, S.H. Duncan, P.O. Sheridan, A.W. Walker, H.J. Flint, Microbial lactate utilisation and the stability of the gut microbiome, Gut Microbiome 3 (2022).
[37] R.A. Jain, The manufacturing techniques of various drug loaded biodegradable poly(lactide-co-glycolide) (PLGA) devices, Biomaterials 21 (2000) 2475–2490.
[38] H.K. Makadia, S.J. Siegel, Poly lactic-co-glycolic acid (PLGA) as biodegradable controlled drug delivery carrier, Polymers (Basel) 3 (2011) 1377–1397.
[39] T. Van de Wiele, P. Van den Abbeele, W. Ossieur, S. Possemiers, M. Marzorati, The simulator of the human intestinal microbial ecosystem (SHIME®), in: K. Verhoeckx, P. Cotter, I. López-Expósito, C. Kleiveland, T. Lea, A. Mackie, T. Requena, D. Swiatecka, H. Wichers (Eds.), The Impact of Food Bioactives on Health: In Vitro and Ex Vivo Models, Springer International Publishing, Cham, 2015, pp. 305–317.

[40] J. Ghyselinck, L. Verstrepen, F. Moens, P. Van den Abbeele, J. Said, B. Smith, I. Bjarnason, A.W. Basit, S. Gaisford, A 4-strain probiotic supplement influences gut microbiota composition and gut wall function in patients with ulcerative colitis, Int. J. Pharm. 587 (2020) 119648.

[41] M. Vertzoni, A. Diakidou, M. Chatzilias, E. Soderlind, B. Abrahamsson, J. B. Dressman, C. Reppas, Biorelevant media to simulate fluids in the ascending colon of humans and their usefulness in predicting intracolonic drug solubility, Pharm. Res. 27 (2010) 2187–2196.

[42] I.A. Neri-Numa, G.M. Pastore, Novel insights into prebiotic properties on human health: a review, Food Res. Int. 131 (2020) 108973.

[43] S. Hoefman, A. Pommerening-Röser, E. Samyn, P. De Vos, K. Heylen, Efficient cryopreservation protocol enables accessibility of a broad range of ammonia-oxidizing bacteria for the scientific community, Res. Microbiol. 164 (2013) 288–292.

[44] M. Vertzoni, E. Kersten, D. van der Mey, U. Muenster, C. Reppas, Evaluating the clinical importance of bacterial degradation of therapeutic agents in the lower intestine of adults using adult fecal material, Eur. J. Pharm. Sci. 125 (2018) 142–150.

[45] E. Karatza, M. Vertzoni, U. Muenster, C. Reppas, The impact of handling and storage of human fecal material on bacterial activity, J. Pharm. Sci. 105 (2016) 3458–3461.

[46] J. Ghyselinck, L. Verstrepen, F. Moens, P. Van Den Abbeele, A. Bruggeman, J. Said, B. Smith, L.A. Barker, C. Jordan, V. Leta, K.R. Chaudhuri, A.W. Basit, S. Gaisford, Influence of probiotic bacteria on gut microbiota composition and gut wall function in an in-vitro model in patients with Parkinson's disease, Int. J. Pharmac. X 3 (2021).

[47] A.J. Marsh, A.-M.A. Yaya, S. Ng, K. Chandrashekhar, J. Roach, S.T. Magness, M. A. Azcarate-Peril, Lumen and mucosa-associated *Lactobacillus rhamnosus* from the intestinal tract of organ donors, Gut Microbiome 1 (2020) e4.

[48] S. Possemiers, I. Pinheiro, A. Verhelst, P. Van den Abbeele, L. Maignien, D. Laukens, S.G. Reeves, L.E. Robinson, T. Raas, Y.-J. Schneider, T. Van de Wiele, M. Marzorati, A dried yeast fermentate selectively modulates both the luminal and mucosal gut microbiota and protects against inflammation, as studied in an integrated in vitro approach, J. Agric. Food Chem. 61 (2013) 9380–9392.

[49] N.M. Tzollas, G.A. Zachariadis, A.N. Anthemidis, J.A. Stratis, A new approach to indophenol blue method for determination of ammonium in geothermal waters with high mineral content, Int. J. Environ. Anal. Chem. 90 (2010) 115–126.

[50] D. Vandeputte, G. Kathagen, K. D'Hoe, S. Vieira-Silva, M. Valles-Colomer, J. Sabino, J. Wang, R.Y. Tito, L. De Commer, Y. Darzi, S. Vermeire, G. Falony, J. Raes, Quantitative microbiome profiling links gut community variation to microbial load, Nature 551 (2017) 507–511.

[51] I. Illumina, MiSeq System Guide, Online, 2018.

[52] J.J. Kozich, S.L. Westcott, N.T. Baxter, S.K. Highlander, P.D. Schloss, Development of a dual-index sequencing strategy and curation pipeline for analyzing amplicon sequence data on the MiSeq Illumina sequencing platform, Appl. Environ. Microbiol. 79 (2013) 5112–5120.

[53] Y. Sambuy, I. De Angelis, G. Ranaldi, M.L. Scarino, A. Stammati, F. Zucco, The Caco-2 cell line as a model of the intestinal barrier: influence of cell and culture-related factors on Caco-2 cell functional characteristics, Cell Biol. Toxicol. 21 (2005) 1–26.

[54] L.E. McCoubrey, A. Favaron, A. Awad, M. Orlu, S. Gaisford, A.W. Basit, Colonic drug delivery: formulating the next generation of colon-targeted therapeutics, J. Control. Release 353 (2022) 1107–1126.

[55] D. Daguet, I. Pinheiro, A. Verhelst, S. Possemiers, M. Marzorati, Arabinogalactan and fructooligosaccharides improve the gut barrier function in distinct areas of the colon in the simulator of the human intestinal microbial ecosystem, J. Funct. Foods 20 (2016) 369–379.

[56] C. Dumrese, L. Slomianka, U. Ziegler, S.S. Choi, A. Kalia, A. Fulurija, W. Lu, D. E. Berg, M. Benghezal, B. Marshall, P.R. Mittl, The secreted *Helicobacter* cysteine-rich protein a causes adherence of human monocytes and differentiation into a macrophage-like phenotype, FEBS Lett. 583 (2009) 1637–1643.

[57] A. Lechanteur, B. Evrard, Influence of composition and spray-drying process parameters on carrier-free DPI properties and behaviors in the lung: a review, Pharmaceutics 12 (2020) 55.

[58] R. Vehring, Pharmaceutical particle engineering via spray drying, Pharm. Res. 25 (2008) 999–1022.

[59] N. Kumskova, Y. Ermolenko, N. Osipova, A. Semyonkin, N. Kildeeva, M. Gorshkova, A. Kovalskii, T. Kovshova, V. Tarasov, J. Kreuter, O. Maksimenko, S. Gelperina, How subtle differences in polymer molecular weight affect doxorubicin-loaded PLGA nanoparticles degradation and drug release, J. Microencapsul. 37 (2020) 283–295.

[60] K.B. Shepard, M.S. Adam, M.M. Morgen, D.M. Mudie, D.T. Regan, J.M. Baumann, D.T. Vodak, Impact of process parameters on particle morphology and filament formation in spray dried Eudragit L100 polymer, Powder Technol. 362 (2020) 221–230.

[61] A. Ekdahl, D. Mudie, D. Malewski, G. Amidon, A. Goodwin, Effect of spray-dried particle morphology on mechanical and flow properties of felodipine in PVP VA amorphous solid dispersions, J. Pharm. Sci. 108 (2019) 3657–3666.

[62] M. Sprengholz, Industrial ram extrusion as innovative tool for the development of biodegradable sustained release implants, in: Faculty for Chemistry and Pharmacy, Ludwig-Maximilians-University, Munich, 2014, p. 178.

[63] A.M. Goula, K.G. Adamopoulos, Effect of maltodextrin addition during spray drying of tomato pulp in dehumidified air: I. Drying kinetics and product recovery, Dry. Technol. 26 (2008) 714–725.

[64] A. Gianfrancesco, C. Turchiuli, E. Dumoulin, S. Palzer, Prediction of powder stickiness along spray drying process in relation to agglomeration, Part. Sci. Technol. 27 (2009) 415–427.

[65] M. Beck-Broichsitter, B. Strehlow, T. Kissel, Direct fractionation of spray-dried polymeric microparticles by inertial impaction, Powder Technol. 286 (2015) 311–317.

[66] F. Wan, F.H. Larsen, H.N. Bordallo, C. Foged, J. Rantanen, M. Yang, Insight into nanoscale network of spray-dried polymeric particles: role of polymer molecular conformation, ACS Appl. Mater. Interfaces 10 (2018) 36686–36692.

[67] F. Wan, A. Bohr, M.J. Maltesen, S. Bjerregaard, C. Foged, J. Rantanen, M. Yang, Critical solvent properties affecting the particle formation process and characteristics of celecoxib-loaded PLGA microparticles via spray-drying, Pharm. Res. 30 (2013) 1065–1076.

[68] F. Wan, M.J. Maltesen, S.K. Andersen, S. Bjerregaard, C. Foged, J. Rantanen, M. Yang, One-step production of protein-loaded PLGA microparticles via spray drying using 3-fluid nozzle, Pharm. Res. 31 (2014) 1967–1977.

[69] Z.E. Ilhan, A.K. Marcus, D.-W. Kang, B.E. Rittmann, R. Krajmalnik-Brown, G. Suen, pH-mediated microbial and metabolic interactions in fecal enrichment cultures, mSphere 2 (2017) e00047-00017.

[70] C. Wischke, S.P. Schwendeman, Principles of encapsulating hydrophobic drugs in PLA/PLGA microparticles, Int. J. Pharm. 364 (2008) 298–327.

[71] J. Siepmann, K. Elkharraz, F. Siepmann, D. Klose, How autocatalysis accelerates drug Release from PLGA-based microparticles: a quantitative treatment, Biomacromolecules 6 (2005) 2312–2319.

[72] D. Rios-Covian, S. Gonzalez, A.M. Nogacka, S. Arboleya, N. Salazar, M. Gueimonde, C.G. de Los Reyes-Gavilan, An overview on fecal branched short-chain fatty acids along human life and as related with body mass index: associated dietary and anthropometric factors, Front. Microbiol. 11 (2020) 973.

[73] J. Gojda, M. Cahova, Gut microbiota as the link between elevated BCAA serum levels and insulin resistance, Biomolecules 11 (2021).

[74] O. Szczesniak, K.A. Hestad, J.F. Hanssen, K. Rudi, Isovaleric acid in stool correlates with human depression, Nutr. Neurosci. 19 (2016) 279–283.

[75] E. Heimann, M. Nyman, A.K. Pålbrink, K. Lindkvist-Petersson, E. Degerman, Branched short-chain fatty acids modulate glucose and lipid metabolism in primary adipocytes, Adipocyte 5 (2016) 359–368.

[76] V.M. Taormina, A.L. Unger, M.R. Schiksnis, M. Torres-Gonzalez, J. Kraft, Branched-chain fatty acids-an underexplored class of dairy-derived fatty acids, Nutrients 12 (2020).

[77] C.K. Yao, J.G. Muir, P.R. Gibson, Review article: insights into colonic protein fermentation, its modulation and potential health implications, Aliment. Pharmacol. Ther. 43 (2016) 181–196.

[78] P. Wang Shui, A. Rubio Luis, H. Duncan Sylvia, E. Donachie Gillian, G. Holtrop, G. Lo, M. Farquharson Freda, J. Wagner, J. Parkhill, P. Louis, W. Walker Alan, J. Flint Harry, Pivotal roles for pH, lactate, and lactate-utilizing bacteria in the stability of a human colonic microbial ecosystem, mSystems 5 (2020), https://doi.org/10.1128/msystems.00645-00620.

[79] B.J. Parker, P.A. Wearsch, A.C.M. Veloo, A. Rodriguez-Palacios, The genus Alistipes: gut Bacteria with emerging implications to inflammation, Cancer, and mental health, Front. Immunol. 11 (2020).

[80] N. Takahashi, J.Z. Xiao, K. Miyaji, T. Yaeshiima, A. Hiramatsu, K. Iwatsuki, S. Kokubo, A. Hosono, Selection of acid tolerant bifidobacteria and evidence for a low-pH-inducible acid tolerance response in *Bifidobacterium longum*, J. Dairy Res. 71 (2004) 340–345.

[81] L. Fontana, M. Bermudez-Brito, J. Plaza-Diaz, S. Muñoz-Quezada, A. Gil, Sources, isolation, characterisation and evaluation of probiotics, Br. J. Nutr. 109 (2013) S35–S50.

[82] Q. Li, Q. Chen, H. Ruan, D. Zhu, G. He, Isolation and characterisation of an oxygen, acid and bile resistant *Bifidobacterium animalis* subsp. lactis Qq08, J. Sci. Food Agric. 90 (2010) 1340–1346.

[83] M. Choroszy, K. Litwinowicz, R. Bednarz, T. Roleder, A. Lerman, T. Toya, K. Kamiński, E. Sawicka-Śmiarowska, M. Niemira, B. Sobieszczańska, Human gut microbiota in coronary artery disease: a systematic review and meta-analysis, Metabolites 12 (2022).

[84] M. Rajilić-Stojanović, W.M. de Vos, The first 1000 cultured species of the human gastrointestinal microbiota, FEMS Microbiol. Rev. 38 (2014) 996–1047.

[85] A. Gorvitovskaia, S.P. Holmes, S.M. Huse, Interpreting Prevotella and Bacteroides as biomarkers of diet and lifestyle, Microbiome 4 (2016) 15.

[86] G.D. Wu, J. Chen, C. Hoffmann, K. Bittinger, Y.-Y. Chen, S.A. Keilbaugh, M. Bewtra, D. Knights, W.A. Walters, R. Knight, R. Sinha, E. Gilroy, K. Gupta, R. Baldassano, L. Nessel, H. Li, F.D. Bushman, J.D. Lewis, Linking long-term dietary patterns with gut microbial enterotypes, Science 334 (2011) 105–108.

[87] P.K.V. Prasoodanan, A.K. Sharma, S. Mahajan, D.B. Dhakan, A. Maji, J. Scaria, V. K. Sharma, Western and non-western gut microbiomes reveal new roles of Prevotella in carbohydrate metabolism and mouth-gut axis, NPJ Biofilms Microbiom. 7 (2021) 77.

[88] D. Statovci, M. Aguilera, J. MacSharry, S. Melgar, The impact of western diet and nutrients on the microbiota and immune response at mucosal interfaces, Front. Immunol. 8 (2017) 838.

[89] T. Liu, L. Zhang, D. Joo, S.-C. Sun, NF-κB signaling in inflammation, Signal Transduct. Target. Therapy 2 (2017) 17023.

[90] C. Gabay, Interleukin-6 and chronic inflammation, Arthritis Res. Ther. 8 (2006) S3.

[91] G. Lopez-Castejon, D. Brough, Understanding the mechanism of IL-1β secretion, Cytokine Growth Factor Rev. 22 (2011) 189–195.

[92] G. van Loo, M.J.M. Bertrand, Death by TNF: a road to inflammation, Nat. Rev. Immunol. 23 (2023) 289–303.

[93] X. Hua, S. Ge, M. Zhang, F. Mo, L. Zhang, J. Zhang, C. Yang, S. Tai, X. Chen, L. Zhang, C. Liang, Pathogenic roles of CXCL10 in experimental autoimmune prostatitis by modulating macrophage chemotaxis and cytokine secretion, Front. Immunol. 12 (2021).
[94] T. Yoshimura, The chemokine MCP-1 (CCL2) in the host interaction with cancer: a foe or ally? Cell. Mol. Immunol. 15 (2018) 335–345.
[95] M.C. Cesta, M. Zippoli, C. Marsiglia, E.M. Gavioli, F. Mantelli, M. Allegretti, R. A. Balk, The role of Interleukin-8 in lung inflammation and injury: implications for the management of COVID-19 and hyperinflammatory acute respiratory distress syndrome, Front. Pharmacol. 12 (2022).
[96] W.I. Khan, Y. Motomura, H. Wang, R.T. El-Sharkawy, E.F. Verdu, M. Verma-Gandhu, B.J. Rollins, S.M. Collins, Critical role of MCP-1 in the pathogenesis of experimental colitis in the context of immune and enterochromaffin cells, Am. J. Physiol. Gastrointest. Liver Physiol. 291 (2006) G803–G811.
[97] A.E. Østvik, A.v. Granlund, M. Bugge, N.J. Nilsen, S.H. Torp, H.L. Waldum, J. K. Damås, T. Espevik, A.K. Sandvik, Enhanced expression of CXCL10 in inflammatory bowel disease: potential role of mucosal toll-like receptor 3 stimulation, Inflamm. Bowel Dis. 19 (2013) 265–274.
[98] M. Wang, Q. Li, C. Shi, J. Lv, Y. Xu, J. Yang, S.L. Chua, L. Jia, H. Chen, Q. Liu, C. Huang, Y. Huang, J. Chen, M. Fang, Oligomer nanoparticle release from polylactic acid plastics catalysed by gut enzymes triggers acute inflammation, Nat. Nanotechnol. 18 (2023) 403–411.
[99] K. Martinez-Guryn, V. Leone, E.B. Chang, Regional diversity of the gastrointestinal microbiome, Cell Host Microbe 26 (2019) 314–324.